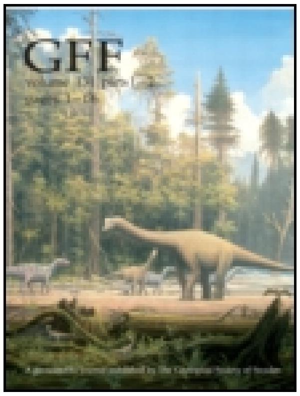

GFF
Publication details, including instructions for authors and subscription information:
http://www.tandfonline.com/loi/sgff20

Intra-orogenic Svecofennian magmatism in SW Finland constrained by LA-MC-ICP-MS zircon dating and geochemistry

Markku Väisänen [a] , Olav Eklund [b] , Yann Lahaye [c] , Hugh O'Brien [c] , Sören Fröjdö [b] , Karin Högdahl [d] & Marjaana Lammi [a]

[a] Department of Geography and Geology, University of Turku, FI-20014, Turku, Finland

[b] Department of Geology and Mineralogy, Åbo Akademi University, FI-20500, Turku, Finland

[c] The Finland Isotope Geosciences Laboratory, Geological Survey of Finland, FI-02151, Espoo, Finland

[d] Department of Earth Sciences, Uppsala University, Villavägen 16, 752 36, Uppsala, Sweden

Version of record first published: 18 Apr 2012

To cite this article: Markku Väisänen, Olav Eklund, Yann Lahaye, Hugh O'Brien, Sören Fröjdö, Karin Högdahl & Marjaana Lammi (2012): Intra-orogenic Svecofennian magmatism in SW Finland constrained by LA-MC-ICP-MS zircon dating and geochemistry, GFF, 134:2, 99-114

To link to this article: http://dx.doi.org/10.1080/11035897.2012.680606

GFF volume 134 (2012), pp. 99–114.
A Scandinavian Journal of Earth Sciences

Article

Intra-orogenic Svecofennian magmatism in SW Finland constrained by LA-MC-ICP-MS zircon dating and geochemistry

MARKKU VÄISÄNEN[1], OLAV EKLUND[2], YANN LAHAYE[3], HUGH O'BRIEN[3], SÖREN FRÖJDÖ[2], KARIN HÖGDAHL[4] and MARJAANA LAMMI[1]

Väisänen, M., Eklund, O., Lahaye, Y., O'Brien, H., Fröjdö, S., Högdahl, K. & Lammi, M., 2012: Intra-orogenic Svecofennian magmatism in SW Finland constrained by LA-MC-ICP-MS zircon dating and geochemistry. *GFF*, Vol. 134 (Pt. 2, June), pp. 99–114. © Geologiska Föreningen. doi: 10.1080/11035897.2012.680606.

Abstract: We have studied plutonic rocks from the Korpo and Rauma areas of south-western Finland which can be categorized as intra-orogenic, i.e. they were intruded during a proposed extensional period between the two main Svecofennian orogenic cycles: the Fennian and Svecobaltic orogenies. The diorite from Rauma yielded an age of 1865 ± 9 Ma and the diorite from Korpo an age of 1852 ± 4 Ma. The adjacent garnet-bearing Korpo granite was 1849 ± 8 Ma in age. Zircons from the granite also included inherited Archaean and older Palaeoproterozic zircons, as well as metamorphic c. 1820 Ma rims. The diorites are high-K to shoshonitic, mantle-derived magmas, rich in Fe, P, F and light rare earth elements. The Korpo granites show typical features of crustal-derived melts and form hybrids with the diorites in contact zones. Both the mantle-derived and crustal-derived intra-orogenic magmatism are considered to have had a causal effect on the subsequent late Svecofennian (Svecobaltic) thermal evolution in southern Finland which culminated in granulite facies metamorphism and large-scale crustal melting.

Keywords: Svecofennian; intra-orogenic; heat source; crustal melting; laser-ablation; zircon.

[1]Department of Geography and Geology, University of Turku, FI-20014 Turku, Finland; markku.vaisanen@utu.fi, taru.lammi@utu.fi
[2]Department of Geology and Mineralogy, Åbo Akademi University, FI-20500 Turku, Finland; olav.eklund@abo.fi, soren.frojdo@abo.fi
[3]The Finland Isotope Geosciences Laboratory, Geological Survey of Finland, FI-02151 Espoo, Finland; yann.lahaye@gtk.fi, hugh.obrien@gtk.fi
[4]Department of Earth Sciences, Uppsala University, Villavägen 16, 752 36 Uppsala, Sweden; karin.hogdahl@geo.uu.se
Manuscript received 22 December 2011. Revised manuscript accepted 23 March 2012.

Introduction

A new tectonic model for the Palaeoproterozoic evolution of the Fennoscandian Shield was presented by Lahtinen et al. (2005). In the model they divided the Svecofennian orogenic evolution in southern Finland into the accretionary Fennian orogeny at 1.92–1.87 Ga, followed by an intra-orogenic extensional period prior to the Svecobaltic continent–continent collision at 1.84–1.79 Ga. This model contradicted the continuous single-stage orogenic model of Gorbatschev & Bogdanova (1993). The proposed intervening intra-orogenic period is challenging to study in the southern Svecofennian terrane of Finland (Fig. 1) because of the extensive tectono-metamorphic events that occurred during the subsequent Svecobaltic stage, i.e. major crustal shortening leading to upright to overturned folding and granulite facies metamorphism with major crustal melting and production of anatectic granites and migmatites (e.g. Ehlers et al. 1993; Korsman et al. 1999). In fact, there are different opinions regarding the existence, magnitude and time constraints of the proposed extensional period and Hermansson et al. (2008) and Saalmann et al. (2009) rather suggested a model of retreating subduction with switching between contractional and extensional periods (c.f. Lahtinen et al. 2005; Cagnard et al. 2007; Nironen & Kurhila 2008; Skyttä & Mänttäri 2008; Torvela et al. 2008; Kukkonen & Lauri 2009; Pajunen et al. 2008; Nironen & Mänttäri 2012).

Suominen (1991) obtained c. 1.86 Ga ages from garnet- and pyroxene-bearing intrusive rocks from Åland, south-west Finland, and considered them to be expressions of intraorogenic magmatism. Van Duin (1992) dated charnockites in the Turku granulite area and interpreted them to be mantle-derived and c. 1.86–1.82 Ga in age, thus adding more examples to this age group. Later, when single grains were studied with the secondary ion mass spectrometer (SIMS) technique at Nordsim, at least the ages of charnockites from the Turku area turned out to be the result of mixed zircon populations, and they were reinterpreted to be synorogenic 1.87 Ga rocks metamorphosed during the late orogenic high heat flow event at c. 1.82 Ga (Väisänen et al. 2002).

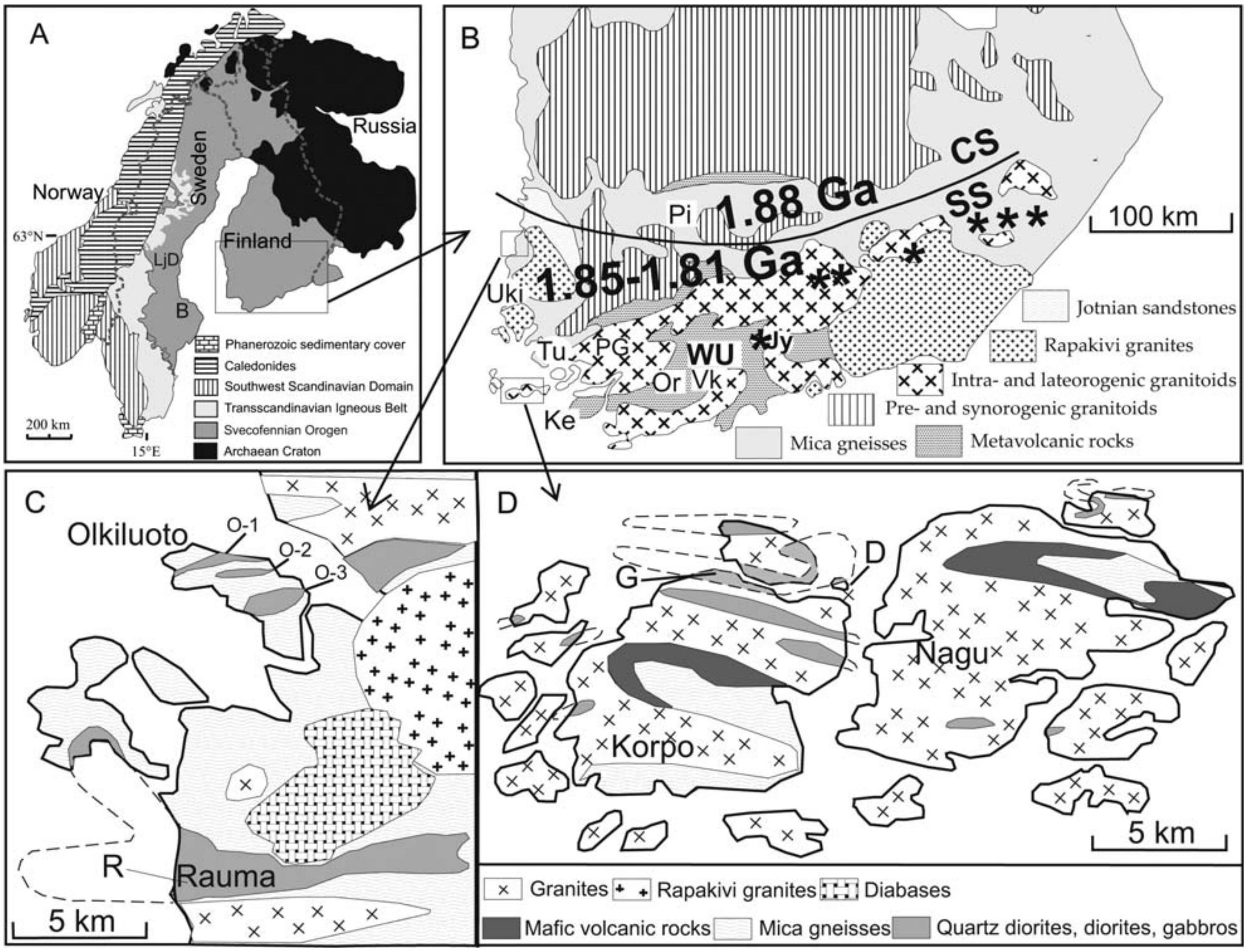

Fig. 1. **A**. General geological map of the Fennoscandian Shield, modified after Högdahl & Sjöström (2001). B, Bergslagen, LjD, Ljusdal Domain. **B**. General geological map of southern Finland, modified after Korsman et al. (1997) with study areas indicated by rectangles C and D, enlarged beneath. "1.88 Ga" and "1.85–1.81 Ga" refer to the dominant ages of metamorphism in the respective areas. CS, Central Svecofennia; Jy, Jyskelä gabbro; Ke, Kemiö; PG, Perniö granite; Pi, Pirkanmaa; SS, Southern Svecofennia; Tu, Turku; Uki, Uusikaupunki; Vk, Västankvarn granite; WU, West Uusimaa; *, intra-orogenic quartzites (Lahtinen & Nironen 2010). **C**. Geological map of the Olkiluoto-Rauma area, modified after Suominen & Torssonen (1993). O-1, O-2 and O-3 indicate Olkiluoto samples Olki-1, Olki-2 and Olki-3, respectively. **D**. Geological map of the Korpo-Nagu area, modified after Suominen (1987). D, Dimanskär (site for the granite dating); G, Galtby (site for the diorite dating); R, Rauma (site for the diorite dating). The extent of the diorites off-shore is shown with dashed lines.

At the time, this seriously threw into question the existence of mantle-derived intra-orogenic magmatism. Lately, however, an increasing number of single zircon age data has revealed that magmatism with ages within the intra-orogenic interval was quite common (Ehlers et al. 2004; Kurhila et al. 2005, 2010; Mänttäri et al. 2006, 2007; Pajunen et al. 2008; Skyttä & Mänttäri 2008). In addition, detrital single zircon age data suggest that sedimentary basins opened at that time, indicating an extensional period (Lahtinen et al. 2002; Bergman et al. 2008). Recently, Lahtinen & Nironen (2010) described weathered paleosols that formed during the same time frame. This strongly supports the idea of two orogenic cycles separated by uplift and erosion during an intra-orogenic period.

In this contribution we present laser-ablation, single zircon age data and whole-rock geochemical data from the plutonic mafic and felsic rocks in the Korpo and Rauma areas, south-western Finland. We suggest that these examples provide evidence for both mantle- and crustal-derived magmatism during an intra-orogenic period within the Palaeoproterozoic Svecofennian orogeny in southern Finland.

Geological background

The Palaeoproterozoic Svecofennian orogen in southern Finland consists of two terranes: Central Svecofennia (CS) and Southern Svecofennia (SS). The position of the boundary between these terranes is not known in detail, but runs approximately E–W c. 120 km north of the south coast, probably along the southern margin of the Pirkanmaa migmatite belt (Fig. 1). The main difference between these terranes is the age of the orogenic events. In CS, the major tectono-metamorphic activities and magmatism took place at c. 1.88 Ga (Nironen 1989; Kilpeläinen 1998; Mouri et al. 1999; Rutland et al. 2004; Lahtinen et al. 2009) and ceased shortly after c. 1.87 Ga when post-kinematic magmas were intruded (Kilpeläinen 1998; Nironen et al. 2000). In SS, the accretionary Fennian stage culminated at c. 1.87 Ga when SS collided with CS, the crust was thickened and synorogenic magmas were intruded (e.g. Nironen 2005). However, the peak tectono-metamorphic events took place later, mainly related to the 1.83–1.81 Ga event (Vaasjoki & Sakko 1988; Ehlers et al. 1993; Korsman et al. 1999; Väisänen et al. 2002;

Mouri et al. 2005; Skyttä & Mänttäri 2008; Mänttäri et al. 2010), now described as the Svecobaltic continent–continent collision (Lahtinen et al. 2005). The latter event strongly reworked and melted the crust and consequently obliterated most primary field evidence of the earlier events.

Our study area is located in south-western Finland within SS (Fig. 1). The 1.90–1.87 Ga bedrock was refolded, high grade metamorphosed and melted (c. 700–800°C at 4–6 kbar; Van Duin 1992; Väisänen & Hölttä 1999; Johannes et al. 2003) at c. 1.83–1.81 Ga in a dextral transpressional tectonic setting (Ehlers et al. 1993; Levin et al. 2005; Stålfors & Ehlers 2006). Recent single zircon datings suggest that high-grade metamorphism started, at least in some places, even earlier at c. 1.85–1.84 Ga (Skyttä & Mänttäri 2008; Torvela et al. 2008; Kurhila et al. 2010; Väisänen et al. 2012). This part of the Svecofennian orogen has been described as an ultra-hot orogen (Chardon et al. 2009).

In Sweden, the possible terrane boundaries are defined along crustal scale shear zones (Högdahl & Sjöström 2001; Korja & Heikkinen 2005; Högdahl et al. 2009; Ogenhall 2010). This might also be the case in Finland, for instance along the south Finland Shear Zone (Torvela & Ehlers 2010).

Study locations

Sampling was done in two study areas in south-west Finland: the Rauma area, that includes the study targets Olkiluoto and Rauma, and the Korpo area (Fig. 1). GPS-coordinates of the sampling sites are shown in Tables 1 and 2.

The *Rauma* samples are from an E–W trending, approximately $2–3 \times 20$ km intrusion that according to the geological map consists of granodiorites and quartz diorites (Suominen & Torssonen 1993). Anatectic granites are also very common in the area. The samples were collected from the city area where the rocks apparently are more mafic than shown on the geological map and will be called diorites in this study. The diorites consist of plagioclase, biotite, hornblende, apatite and quartz, titanite and opaques are accessories. The plagioclase is sericitized. The rock is folded, migmatized and displays a steep E–W trending tectonic foliation.

Olkiluoto, 10 km N of Rauma city, is the location of a nuclear power plant and the Finnish nuclear waste disposal site. The bedrock of Olkiluoto has been mapped and studied in considerable detail, including dating (e.g. Mattila et al. 2008). We collected samples from rocks that had previously been described as tonalitic gneisses and dated by the U–Pb single zircon SIMS method. Their concordia ages and the original sample numbers are 1863 ± 6 Ma (A1819), 1856 ± 5 Ma (A1880) and 1851 ± 5 Ma (A1879; Mänttäri et al. 2006, 2007). The corresponding samples collected for geochemical analyses are Olki-1, Olki-2 and Olki-3, respectively (Table 2). The rocks occur as narrow dyke-like intrusions, tens to hundreds of metres wide. They consist of varying amounts of plagioclase, biotite, hornblende and quartz, with accessory apatite and monazite/zircon. The full petrographic descriptions of the samples are given in Mänttäri et al. (2006, 2007). Geochemically, they are more basic than their previous rock names implied and will also be called diorites in this study.

The *Korpo* diorites occur in the northern part of the island of Korpo covering an area of c. 5×10 km. They comprise several E–W trending intrusions which show distinct anomalies on aeromagnetic maps. The diorites consist of plagioclase, hornblende, biotite, apatite, K-feldspar, some quartz, titanite, opaques and zircon. The diorites are surrounded by pink, porphyritic granites which are the main rock types of the area (Suominen 1987). The granites consist of K-feldspar, quartz, plagioclase, garnet and biotite, with some accessory zircon. The plagioclase is sericitized and the garnet has clorite-filled cracks. The diorites are folded and display a steep E–W trending tectonic foliation. The largest of these bodies forms a folded structure with a subhorizontal contact to the granite in the fold hinge indicating that the intrusion originally was a subhorizontal sheet (e.g. Ehlers et al. 1993; Figs. 1D and 2A) with an estimated thickness of c. 500 m. The diorites and granites also form hybrids where they are in contact (Fig. 2B). Granites dominate at the island of Nagu, east of Korpo, but many small mafic "inclusions" are shown on the geological map (Edelman 1973). One of these shows quite a strong positive anomaly on the aeromagnetic map, much larger than the exposed mafic body, indicating a larger volume of mafic rocks at depth below the granite.

Analytical methods

Zircons for the U–Pb analyses were separated using a shaking table, hand magnet, heavy liquids, Franz magnetic separator and hand picking. The grains were mounted on an epoxy disc. The disc was ground down to remove a half thickness of the grains to expose grain interiors, then polished. The zircons were imaged with back-scattered electrons (BSE) at Topanalytica Ltd., Turku, Finland.

U–Pb isotope analyses were done utilizing the Nu Plasma high resolution multicollector inductively coupled plasma mass spectrometer (ICP-MS) together with a New Wave UP193 neodymium-doped yttrium aluminium garnet (Nd:YAG) laser microprobe at the Geological Survey of Finland, Espoo. Samples were ablated in He gas (gas flow = 0.2–0.3 l/min) using a low volume teardrop-shaped ($< 2.5\,cm^3$) laser ablation cell (Horstwood et al. 2003). The He aerosol was mixed with Ar (gas flow = 1.2 l/min) in a Teflon mixing cell prior to entry into the plasma. The gas mixture was optimized daily for maximum sensitivity. All analyses were made in static ablation mode. Ablation conditions were beam diameter 25 μm, pulse frequency 10 Hz and beam energy density $1.4\,J/cm^2$. A single U–Pb measurement included 30 s of on-mass background measurement, followed by 60 s of ablation with a stationary beam. Masses 204, 206 and 207 were measured in secondary electron multipliers, and mass 238 in the extra high mass Faraday collector. The geometry of the collector block does not allow simultaneous measurement of ^{208}Pb and ^{232}Th. Ion counts were converted and reported as volts by the Nu Plasma time-resolved analysis software. ^{235}U was calculated from the signal at mass 238 using a natural $^{238}U/^{235}U = 137.88$. Mass number 204 was used as a monitor for common ^{204}Pb. In an ICP-MS analysis, ^{204}Hg originates mainly from the He supply. The observed background counting rate on mass 204 was c. 1200 (c. 1.3×10^{-5} V), and had been stable at that level during the year prior to the measurements. The contribution of ^{204}Hg from the plasma was eliminated by on-mass background measurement prior to each analysis. Age-related common lead (Stacey & Kramers 1975) correction was used if the analysis showed common Pb contents above the detection limit. Signal strengths on mass 206 were typically $> 10^{-3}$ V, depending on the U content and age of the zircon. Two calibration standards were run in duplicate at the beginning and end of each analytical session, and at regular intervals during sessions. Raw data were corrected for

Table 1. LA-MC-ICP-MS zircon U–Pb data from plutonic rocks in the Rauma and Korpo areas, south-west Finland.

Name	U (ppm)	^{206}Pb (ppm)	$^{206}Pb_c$ (%)[a]	$^{206}Pb/^{204}Pb$	$^{207}Pb/^{206}Pb$	1σ[b]	$^{207}Pb/^{235}U$	1σ[b]	$^{206}Pb/^{238}U$	1σ[b]	ρ[c]	Central (%)[d]	$^{207}Pb/^{206}Pb$	1σ[b]	$^{207}Pb/^{235}U$	1σ[b]	$^{206}Pb/^{238}U$	1σ[b]
Sample Rauma diorite (14-MJV-08). National coordinates: North = 6,793,733, East = 3,202,829																		
Rauma-10	529	188	0.00	83,118	0.1131	0.0016	5.33	0.35	0.342	0.022	0.98	2.8	1850	26	1874	56	1895	104
Rauma-16	391	136.7	4.70×10^{-2}	57,023	0.1135	0.0016	5.24	0.34	0.334	0.021	0.98	0.2	1857	25	1858	55	1860	101
Rauma-16b	520	186.2	1.70×10^{-2}	56,287	0.1134	0.0016	5.37	0.35	0.344	0.022	0.98	3.1	1854	25	1881	56	1905	105
Rauma-17	214	75.9	2.6×10^{-2}	26,330	0.1140	0.0016	5.36	0.35	0.341	0.022	0.98	1.6	1865	25	1878	56	1890	105
Rauma-18	154	52.4	7.60×10^{-2}	16,703	0.1142	0.0016	5.10	0.33	0.324	0.020	0.97	−3.5	1867	25	1837	54	1810	98
Rauma-20	187	64.3	0.00	24,727	0.1140	0.0016	5.21	0.34	0.332	0.021	0.98	−1	1863	24	1854	55	1846	101
Rauma-22	248	86.5	5.50×10^{-2}	29,050	0.1136	0.0016	5.24	0.34	0.335	0.021	0.98	0.2	1858	24	1860	55	1862	102
Rauma-26	459	168	1.90×10^{-2}	76,385	0.1135	0.0016	5.45	0.36	0.348	0.023	0.98	4.4	1857	26	1893	57	1927	108
Rauma-24	247	92.5	0.00	41,146	0.1142	0.0016	5.60	0.38	0.355	0.024	0.98	5.8	1867	26	1915	59	1960	113
Rauma-29	351	120.5	1.10×10^{-2}	49,422	0.1136	0.0016	5.19	0.34	0.331	0.021	0.98	−0.8	1858	26	1851	55	1845	102
Rauma-28	277	95.3	1.90×10^{-2}	28,520	0.1137	0.0016	5.16	0.33	0.329	0.021	0.98	−1.6	1860	25	1846	55	1834	100
Rauma-30	315	108.8	1.50×10^{-1}	43,584	0.1134	0.0016	5.20	0.34	0.333	0.021	0.98	−0.2	1854	26	1852	55	1851	102
Rauma-31	300	105.6	0.00	63,972	0.1139	0.0016	5.30	0.35	0.338	0.022	0.98	0.8	1863	24	1870	56	1876	104
Rauma-32	293	102.1	1.30×10^{-2}	32,655	0.1139	0.0016	5.25	0.34	0.334	0.021	0.98	−0.2	1863	24	1861	56	1860	103
Rauma-34	122	41.7	4.10×10^{-2}	12,614	0.1147	0.0017	5.21	0.34	0.329	0.021	0.98	−2.4	1876	24	1855	55	1836	101
Rauma-34b	153	53.9	2.70×10^{-2}	26,195	0.1145	0.0017	5.30	0.35	0.336	0.021	0.98	−0.3	1872	24	1869	56	1867	104
Rauma-35	149	51.5	1.70×10^{-2}	16,373	0.1144	0.0017	5.26	0.34	0.334	0.021	0.98	−0.9	1870	26	1863	56	1856	103
Rauma-38	355	121.1	1.20×10^{-1}	23,695	0.1149	0.0017	5.15	0.33	0.325	0.020	0.97	−3.9	1879	26	1845	55	1815	99
Rauma-39	284	96.8	0.00	31,373	0.1129	0.0016	5.09	0.33	0.327	0.021	0.98	−1.5	1847	25	1835	55	1824	100
Rauma-39b	165	57	1.20×10^{-1}	15,680	0.1138	0.0016	5.20	0.34	0.331	0.021	0.98	−1	1860	25	1852	55	1844	102
Rauma-40	385	133.9	1.10×10^{-1}	28,494	0.1141	0.0017	5.22	0.34	0.332	0.021	0.98	−1.2	1866	26	1855	55	1846	102
Rauma-41	935	326.6	1.10×10^{-2}	75,316	0.1148	0.0017	5.25	0.34	0.332	0.021	0.98	−1.9	1877	26	1861	55	1846	102
Rauma-44	285	101.1	5.60×10^{-2}	28,032	0.1143	0.0017	5.36	0.35	0.340	0.022	0.98	1.1	1869	26	1878	57	1886	106
Rauma-43	145	50.4	0.00	17,834	0.1149	0.0017	5.26	0.34	0.332	0.021	0.98	−1.8	1878	25	1863	56	1849	103
Rauma-45	372	128.2	2.40×10^{-2}	123,154	0.1143	0.0017	5.19	0.34	0.329	0.021	0.98	−2.1	1869	25	1851	55	1835	101
Rauma-45b	267	94.1	3.50×10^{-2}	24,540	0.1145	0.0017	5.32	0.35	0.337	0.022	0.98	.	1872	24	1872	56	1872	104
Rauma-47	217	73	0.00	29,633	0.1147	0.0016	5.40	0.31	0.341	0.019	0.97	1.2	1875	24	1885	49	1894	92
Rauma-49	499	174.2	3.30×10^{-2}	71,084	0.1132	0.0016	5.51	0.32	0.353	0.020	0.97	6	1852	24	1902	50	1948	96
Rauma-49b	606	209.6	3.30×10^{-2}	47,219	0.1141	0.0016	5.49	0.32	0.349	0.020	0.97	4.1	1865	25	1900	50	1931	94
Rauma-50	699	242.8	1.3×10^{-3}	111,639	0.1141	0.0016	5.51	0.32	0.350	0.020	0.97	4.3	1866	24	1902	50	1936	95
Rauma-52a	193	68.2	2.40×10^{-2}	22,105	0.1148	0.0016	5.69	0.34	0.359	0.021	0.97	6.2	1877	24	1929	51	1978	98
Rauma-52b	313	106.6	1.10×10^{-2}	47,975	0.1139	0.0016	5.41	0.31	0.344	0.019	0.97	2.8	1863	25	1886	49	1908	93
Sample Korpo diorite (29-MJV-07; Galtby). National coordinates: North = 6,687,096, East = 3,200,050																		
Galtby1	115	32.2	0.00	17,499	0.11406	0.00067	5.20	0.12	0.3306	0.0071	0.97	−1.5	1865	10	1852	19	1841	35
Galtby2	143	40	0.00	20,382	0.11391	0.00066	5.22	0.11	0.3321	0.0068	0.96	−0.9	1863	10	1855	18	1849	33
Galtby3	130	36.3	0.00	23,670	0.11368	0.00066	5.19	0.11	0.3310	0.0070	0.97	−1	1859	10	1851	19	1843	34
Galtby4	169	46.5	8.20×10^{-2}	18,572	0.11309	0.00064	5.12	0.11	0.3285	0.0069	0.97	−1.2	1850	10	1840	18	1831	33
Galtby5	146	40.3	3.50×10^{-2}	20,138	0.11335	0.00067	5.12	0.12	0.3279	0.0071	0.97	−1.6	1854	10	1840	19	1828	35
Galtby6	301	83.4	6.70×10^{-3}	123,214	0.11331	0.00065	5.20	0.12	0.3325	0.0072	0.97	−0.2	1853	10	1852	19	1851	35
Galtby7	115	31.3	5.30×10^{-3}	18,674	0.11403	0.00068	5.18	0.12	0.3295	0.0072	0.96	−1.8	1865	10	1850	19	1836	35
Galtby8	136	37	1.30×10^{-1}	18,336	0.11293	0.00068	5.11	0.11	0.3281	0.0069	0.96	−1.1	1847	11	1838	19	1829	34
Galtby9	108	28.9	7.40×10^{-2}	13,334	0.11334	0.00067	5.08	0.11	0.3252	0.0068	0.96	−2.4	1854	11	1833	18	1815	33
Galtby10	157	43	0.00	24,949	0.11352	0.00065	5.21	0.12	0.3327	0.0074	0.97	−0.3	1856	10	1854	19	1851	36
Galtby11	184	49.9	1.70×10^{-2}	29,153	0.11321	0.00067	5.17	0.12	0.3309	0.0071	0.96	−0.6	1852	10	1847	19	1843	35
Galtby12	91	24.6	8.10×10^{-2}	12,866	0.11338	0.00068	5.15	0.12	0.3291	0.0071	0.96	−1.2	1854	11	1844	19	1834	34
Galtby13	132	34.9	7.20×10^{-2}	14,948	0.11326	0.00068	5.04	0.11	0.3229	0.0067	0.96	−3	1852	10	1826	18	1804	33
Galtby14	135	35.3	0.00	21,448	0.11399	0.00069	5.05	0.10	0.3214	0.0063	0.96	−4.1	1864	10	1828	17	1797	31
Galtby15	290	80.2	2.70×10^{-2}	43,488	0.11324	0.00067	5.29	0.11	0.3391	0.0071	0.96	1.9	1852	11	1868	19	1882	34
Galtby16	253	68.1	2.00×10^{-1}	14,995	0.11279	0.00071	5.18	0.11	0.3333	0.0070	0.96	0.6	1845	11	1850	19	1854	34
Galtby17	124	31.8	4.60×10^{-2}	34,650	0.11286	0.00070	5.00	0.11	0.3215	0.0066	0.96	−3	1846	11	1820	18	1797	32
Galtby18	339	91.8	3.90×10^{-2}	51,346	0.11238	0.00067	5.21	0.11	0.3360	0.0070	0.96	1.8	1838	11	1854	18	1867	34
Galtby19	151	40.9	8.60×10^{-1}	3602	0.11343	0.00075	5.24	0.11	0.3352	0.0069	0.95	0.5	1855	12	1860	18	1864	33
Galtby20	137	36.3	8.80×10^{-3}	29,723	0.11360	0.00069	5.17	0.11	0.3299	0.0067	0.96	−1.2	1858	11	1847	18	1838	33
Galtby21	177	48.1	0.00	51,635	0.11303	0.00068	5.29	0.12	0.3394	0.0073	0.96	2.2	1849	11	1867	19	1884	35
Galtby22	280	74.5	0.00	116,734	0.11247	0.00068	5.26	0.12	0.3393	0.0075	0.97	2.7	1840	11	1863	19	1883	36
Galtby23	275	74.3	4.90×10^{-2}	36,681	0.11265	0.00068	5.27	0.12	0.3391	0.0071	0.96	2.5	1843	11	1864	19	1882	34
Galtby24	325	88	3.20×10^{-2}	34,250	0.11233	0.00068	5.29	0.12	0.3414	0.0072	0.96	3.5	1837	11	1867	19	1893	34
Galtby25	291	79.1	2.50×10^{-2}	31,441	0.11276	0.00069	5.33	0.12	0.3430	0.0072	0.96	3.6	1844	11	1874	19	1901	34
Galtby26	249	65.9	0.00	42,080	0.11279	0.00072	5.18	0.13	0.3329	0.0084	0.97	0.5	1845	11	1849	22	1853	40

Table 1. (Contd.)

Name	U (ppm)	^{206}Pb (ppm)	$^{206}Pb_c$ (%)[a]	$^{206}Pb/^{204}Pb$	$^{207}Pb/^{206}Pb$	1σ[b]	$^{207}Pb/^{235}U$	1σ[b]	$^{206}Pb/^{238}U$	1σ[b]	ρ[c]	Central (%)[d]	$^{207}Pb/^{206}Pb$	1σ[b]	$^{207}Pb/^{235}U$	1σ[b]	$^{206}Pb/^{238}U$	1σ[b]
Galtby27	91	23.8	3.90×10^{-2}	14,279	0.11385	0.00071	5.19	0.11	0.3304	0.0069	0.96	− 1.3	1862	11	1850	19	1840	33
Galtby-58	201	65.1	2.90×10^{-2}	44,980	0.1135	0.0016	5.14	0.29	0.329	0.018	0.97	− 1.5	1856	23	1843	48	1831	87
Galtby-62	125	40.2	7.90×10^{-2}	13,344	0.1137	0.0016	5.12	0.29	0.327	0.018	0.97	− 2.3	1860	23	1840	48	1823	87
Sample Korpo granite (6-MJV-08; Dimanskär). National coordinates: North = 6,686,818, East = 3,205,158																		
Dima2-1a	539	173.9	0	79,018	0.1130	0.0013	5.33	0.17	0.342	0.010	0.94	3.1	1848	20	1874	28	1897	50
Dima2-1b	561	188.6	0.0037	191,643	0.1128	0.0010	5.25	0.16	0.3373	0.0098	0.95	1.8	1845	16	1860	26	1874	47
Dima2-3	778	260.4	0.0038	113,278	0.1138	0.0013	5.37	0.16	0.3424	0.0090	0.91	2.3	1860	21	1880	25	1898	43
Dima2-3b	799	264	0	126,668	0.1143	0.0013	5.36	0.17	0.3405	0.0098	0.93	1.3	1868	20	1879	27	1889	47
Dima2-4	408	139.8	0.043	33,114	0.1135	0.0010	5.28	0.13	0.3372	0.0079	0.94	1.1	1856	16	1865	21	1873	38
Dima2-6	337	108.2	0	40,694	0.1124	0.0013	5.18	0.16	0.3339	0.0096	0.93	1.2	1839	20	1849	26	1857	46
Dima2-6b	477	145.6	0.17	24,530	0.1130	0.0014	5.18	0.18	0.333	0.011	0.94	0.2	1848	22	1849	30	1851	54
Dima2-7	580	193	0.01	435,223	0.1134	0.0013	5.40	0.16	0.34521	0.0094	0.92	3.5	1855	20	1885	25	1912	45
Dima-8	212	67.6	0.31	11,385	0.1146	0.0014	5.19	0.14	0.3286	0.0082	0.90	−2.6	1874	21	1852	24	1832	40
Dima-9	695	224.7	0.015	87,533	0.1124	0.0013	5.21	0.15	0.3362	0.0087	0.92	1.8	1839	20	1854	24	1868	42
Dima-12	995	314.3	0.039	79,717	0.1124	0.0013	5.32	0.14	0.3434	0.0084	0.91	4.1	1838	20	1872	23	1903	40
Dima-13	705	224.9	0.099	26,581	0.1121	0.0013	5.34	0.16	0.3453	0.0093	0.93	4.9	1834	20	1875	25	1912	45
Dima-14	416	136.5	0.025	61,883	0.1129	0.0013	5.37	0.17	0.3451	0.0099	0.93	4	1847	21	1881	26	1911	47
Dima-15	625	192.3	0.1	24,329	0.1106	0.0013	5.34	0.18	0.350	0.011	0.94	8	1809	20	1875	29	1935	54
Dima 2x	683	376.9	0.052	11,679	0.1120	0.0007	5.36	0.16	0.347	0.010	0.98	5.5	1832	11	1878	25	1919	48
Dima 7x	773	389.8	0	183,575	0.1120	0.0006	5.20	0.25	0.337	0.016	0.99	2.4	1833	10	1853	42	1872	79
Dima 1	*743*	*298.8*	*2*	*1308*	*0.1114*	*0.0018*	*3.95*	*0.21*	*0.257*	*0.013*	*0.95*	*− 21.3*	*1823*	*29*	*1625*	*42*	*1476*	*65*
Dima-5z	*738*	*393.5*	*0.086*	*31,406*	*0.11134*	*0.00061*	*5.38*	*0.30*	*0.351*	*0.020*	*1.00*	*7.4*	*1821*	*10*	*1882*	*48*	*1938*	*94*
Dima-10	*754*	*249.2*	*0.02*	*68,537*	*0.1113*	*0.0012*	*5.32*	*0.18*	*0.347*	*0.011*	*0.94*	*6.2*	*1821*	*19*	*1872*	*28*	*1919*	*52*
Dima-15	*625*	*192.3*	*0.1*	*24,329*	*0.1106*	*0.0013*	*5.34*	*0.18*	*0.350*	*0.011*	*0.94*	*8*	*1809*	*20*	*1875*	*29*	*1935*	*54*
Dima 16	*724*	*376.1*	*0.0084*	*62,482*	*0.11162*	*0.00066*	*5.43*	*0.27*	*0.353*	*0.018*	*0.99*	*7.7*	*1826*	*10*	*1889*	*43*	*1947*	*84*
Dima2-2	**462**	**151.7**	**0.024**	**56,400**	**0.1167**	**0.0011**	**5.22**	**0.15**	**0.3244**	**0.0086**	**0.95**	**− 5.7**	**1907**	**16**	**1856**	**24**	**1811**	**42**
Dima 8x	**1014**	**754.4**	**0**	**126,153**	**0.1743**	**0.0011**	**11.84**	**0.44**	**0.493**	**0.018**	**0.99**	**− 0.8**	**2599**	**10**	**2592**	**35**	**2583**	**78**
Dima2-5	121	51.2	2.1	992	0.1082	0.0015	6.05	0.24	0.406	0.015	0.94	28.5	1769	25	1983	35	2195	71
Dima-11	1451	381.4	0.065	34,323	0.1023	0.0010	3.79	0.10	0.2686	0.0063	0.93	− 8.9	1666	17	1590	20	1534	32
Dima-8b	662	190.4	9.5	191	0.0956	0.0036	3.51	0.16	0.2666	0.0067	0.56	− 1.1	1539	70	1530	36	1523	34
dima 5x	903	431	0.24	16,456	0.1086	0.0006	4.67	0.28	0.312	0.018	1.00	− 1.7	1776	11	1762	49	1749	90
Dima 16b-a	708	289.3	4.7	326	0.1209	0.0029	4.36	0.19	0.2615	0.0095	0.84	− 26.8	1969	41	1704	36	1497	49

Note: Analyses indicated by italics were used for age calculations from zircon rims. Analyses indicated by bold are inferred to be inherited and omitted from age calculation. Analyses indicated by underline were omitted from concordia age calculation on the basis discussed in the text.

[a] Percentage of common 206Pb in measured 206Pb calculated from the 204Pb signal using age-related common lead after model by Stacey & Kramers (1975).

[b] Errors are absolute 1σ values.

[c] Error correlation for $^{207}Pb/^{235}U$ versus $^{206}Pb/^{238}U$ ratios.

[d] The percentage of discordance from the concordia, relative to the centroid of the ellipse.

Table 2. Geochemical analyses of plutonic rocks from Rauma, Olkiluoto and Korpo, south-west Finland.

Sample	3-MJV-07	4-MJV-07	14-MJV-08	15-MJV-08	17-MJV-08	19-MJV-08	20-MJV-08	22-MJV-08	29-MJV-07	4-MJV-08	7-MJV-08	9.1-MJV-08	9.2-MJV-08	26-MJV-08	31-MJV-08	5-MJV-08	23-MJV-08	6-MJV-08	24-MJV-08	OLKI-1-08	OLKI-2-08	OLKI-3-08
Locality	Rauma	Rauma	Rauma	Rauma	Rauma	Rauma	Rauma	Rauma	Korpo	Korpo	Korpo	Korpo	Korpo	Korpo	Korpo	Korpo	Korpo	Korpo	Korpo	Olkiluoto	Olkiluoto	Olkiluoto
N-coordinate[a]	6,793,342	6,793,813	6,793,733	6,793,635	6,794,355	6,794,628	6,793,829	6,791,889	6,687,096	6,686,978	6,687,102	6,687,536	6,687,536	6,686,707	6,684,559	6,687,022	6,684,272	6,686,818	6,684,702	6,805,464	6,804,057	6,805,330
E-coordinate[a]	3,203,701	3,202,569	3,202,829	3,202,646	3,204,812	3,202,823	3,203,208	3,203,632	3,200,050	3,205,230	3,204,555	3,198,955	3,198,955	3,202,841	3,205,600	3,205,209	3,205,314	3,205,158	3,205,166	3,201,324	3,205,438	3,203,943
Rock type[b]	Dr	Dr	Dr	Dr	Dr	Dr	Dr	Dr	Dr	Dr	Dr	Dr	Dr	Dr	Dr	Hy	Hy	Gr	Gr	Dr	Dr	Dr
SiO_2	55.41	55.48	51.69	53.94	50.6	57.46	54.26	59.74	53.06	55.67	53.34	47.2	50.06	54.84	47.55	65.36	62.95	71.43	71.63	55.48	60.24	48.75
Al_2O_3	15.75	16.11	18.62	16.35	15.25	16.04	17.58	16.29	15.86	15.5	16.83	15.97	15.02	15.92	17.18	14.25	14.91	14.19	13.82	16.71	16.47	16.45
Fe_2O_3	8.92	9.31	9.6	9.2	10.26	9.39	7.79	7.68	10.95	9.37	10.74	14.13	11.56	10.35	15.9	5.85	8.16	2.59	3.18	7.84	7.05	11.47
MgO	4.07	3.74	3.57	4.23	4.84	2.85	4.92	2.63	3.46	3.16	2.86	4.43	5.61	3.1	3.24	1.93	1.84	0.41	0.51	4.4	2.82	6.11
CaO	5.43	5.76	5.67	5.09	7.57	4.88	6.22	4.27	6.46	5.27	5.9	7.19	7.96	5.89	4.11	3.43	3.05	0.88	1.28	4.73	4.08	7.25
Na_2O	3	3.04	3.57	2.52	3.25	2.07	3.44	2.84	3.88	3.1	3.83	3.39	3.33	3.29	3.49	3.13	3.24	2.54	2.93	3.32	2.85	2.65
K_2O	3.01	2.74	2.96	3.2	2.16	3.27	2.54	2.9	2.17	4.2	2.43	2.5	1.69	2.5	4.09	3.52	3.27	6.85	5.59	2.56	2.9	1.87
TiO_2	2.02	1.55	1.83	1.99	3.37	1.93	0.86	1.37	1.66	1.52	1.74	2.2	2.21	1.71	1.96	0.87	1.1	0.3	0.27	1.04	1	1.68
P_2O_5	1.142	1.03	0.91	1.1	1.87	0.92	0.7	0.79	0.974	0.61	0.84	1.38	0.95	0.94	1.13	0.24	0.38	0.13	0.11	0.67	0.55	1.88
MnO	0.11	0.12	0.14	0.1	0.12	0.1	0.11	0.04	0.14	0.11	0.15	0.17	0.16	0.12	0.12	0.06	0.12	0.02	0.03	0.1	0.09	0.13
Mg#[c]	47.5	44.3	42.4	47.7	48.3	37.6	55.6	40.4	38.5	40.1	34.5	38.3	49	37.2	28.8	39.5	30.9	23.9	24.1	52.6	44.2	51.3
Sc	13	15	17	14	16	14	12	11	17	20	15	20	20	13	16	9	17	2	4	14	12	17
Ba	807	871	1298	796	651	986	655	1126	802	812	460	852	629	810	482	661	848	673	607	589	869	665
Cs	3.4	3.9	4.4	5.3	1.7	5.1	1.9	2.3	0.8	0.7	1.2	0.8	0.4	1.2	3.5	0.4	1.6	0.6	0.8	2.7	5.9	1.4
Hf	6.3	6.7	12.4	6.4	5.4	8.3	5.7	9	6.2	9.4	9.9	6.2	4.7	7.2	6.9	6.2	12.4	7.3	5.2	5.7	8	3.3
Nb	22.9	24	48	27.4	25.4	33.6	18.3	28	31.3	29.9	64.5	35.1	19	27.9	42.1	14.1	40.3	10.5	13.1	21.2	30.1	15.8
Rb	103.9	119.5	134.5	136.7	58.3	164.4	80.4	158.9	69.4	133.4	118.8	79.9	46.6	109.2	257.6	127.9	166.7	185.1	164.2	88.8	147.4	50.4
Sr	1059	1122	1294.1	925.9	1236.4	836	1013.3	1177.3	1323	587.8	660.4	1124.2	1452.7	1103.7	420.8	542.8	445.8	137.5	239.4	859.3	692.6	1437.7
Ta	1.1	1.5	3.5	1.3	1.3	1.7	0.8	1.4	1.2	1.7	2.4	1.5	1.2	1.1	1.6	0.7	1.5	0.3	0.4	1.1	2	0.8
Th	7.7	5.3	9.8	7.2	4.1	7.4	5.7	14.1	6.4	12.9	7.9	5.8	4	12.2	6.7	9.5	34.9	53.9	37.3	6.7	9	2.6
U	2.7	3.7	3.6	3.2	2.1	4.1	2.1	4.7	1.1	1.2	1.4	1	1.5	1.1	2.4	0.8	2.8	3.8	6.5	2.8	3.9	1.4
V	127	126	134	128	159	109	99	92	103	107	75	130	126	96	192	56	53	12	12	158	94	255
Zr	276.6	314.4	580.4	291.2	245.6	352	249.5	405.4	275.8	325.9	432.1	256.5	182.4	308.9	272.8	224.4	505.9	222.2	193.9	228.2	325.2	144.5
Y	21.5	25.5	37.2	22.8	23.2	27.3	18.3	21.1	35.5	48.8	76.1	46.2	27.7	30.5	59.2	20	40.7	9.8	8.5	19.3	26.6	25.2
La	67.7	65.4	82.4	63.5	62.3	65.8	55.1	117.6	96.9	76.8	74.1	88.2	70	84.1	57.3	54.8	157.2	84	59.8	58.8	79.7	73.1
Ce	149.3	143.8	200	146.4	144.6	151.9	117.5	245.1	205.1	172.2	154.3	203.4	159.6	179	132.2	115.7	306.9	177.2	123.8	117.5	162	158
Pr	18.45	18.87	25.65	18.84	19.02	19.99	14.4	29.37	25.76	24.29	21.57	27.14	20.93	22.21	18.94	13.76	34.48	21.51	14.18	14.87	20.2	21.84
Nd	71.4	74.5	100.7	74.9	78.1	81.1	54.8	105.2	103.6	92.7	87.4	106.4	80.6	84.7	77.9	49.6	122	76.5	50.5	53.7	74.4	86.2
Sm	11.03	11.57	16.75	11.6	12.27	12.74	8.27	13.51	14.52	17.4	19.33	17.46	12.84	12.46	18.33	8.04	17.15	13.17	7.17	8.42	11.03	13.79
Eu	2.75	3.02	4.52	3.17	3.33	3.35	2.08	2.46	3.03	2.22	2.37	3.3	3.21	2.67	1.72	1.37	1.68	0.85	0.92	2.18	2.49	3.1
Gd	7.37	8.13	13.08	8.98	10.18	10.39	6.48	9.87	11.01	14.51	19.51	12.81	9.05	10.56	17.31	5.69	14.75	8.25	5.27	6.59	8.29	10.31
Tb	0.98	1.05	1.54	1.05	1.1	1.22	0.76	1	1.5	2.05	3.21	1.79	1.22	1.31	2.58	0.81	1.73	0.87	0.53	0.79	1.04	1.16
Dy	4.55	4.86	7.37	4.65	5.21	6.14	3.55	4.45	7.49	9.21	16.31	8.71	5.82	6.13	12.31	3.9	8.65	3.02	2.28	3.67	4.89	4.69
Ho	0.74	0.83	1.24	0.8	0.83	1.07	0.68	0.73	1.33	1.71	3.04	1.49	0.97	1.03	1.98	0.68	1.49	0.31	0.33	0.66	0.93	0.89
Er	1.86	2.15	3.47	2.03	2.06	2.61	1.76	1.97	3.36	4.5	7.42	4.06	2.39	2.69	4.74	1.74	3.71	0.54	0.68	1.89	2.51	2.32
Tm	0.28	0.31	0.56	0.31	0.3	0.38	0.26	0.28	0.47	0.65	0.96	0.57	0.34	0.39	0.54	0.25	0.53	0.07	0.09	0.27	0.4	0.33
Yb	1.6	1.94	3.35	1.8	1.73	2.22	1.65	1.58	2.78	3.91	4.97	3.26	2.02	2.18	2.83	1.49	2.93	0.44	0.59	1.68	2.5	2.01
Lu	0.25	0.28	0.48	0.26	0.23	0.3	0.24	0.24	0.37	0.51	0.64	0.46	0.27	0.32	0.36	0.21	0.42	0.07	0.09	0.25	0.35	0.26
Cu	53.2	62.1	29.9	44.5	58.3	31.7	44.1	99.8	25.5	25.2	29.8	29.4	35	32.2	3.8	12.2	20.7	4.5	4.9	36.1	38.7	60
Pb	7.9	9.5	3.9	2.1	2.8	4.4	2.8	4.4	9.3	2.8	2.3	5.2	4	4	3.1	5.8	4.4	18.1	6.5	8.4	4	3.3
Zn	115	91	116	107	82	125	90	159	140	74	144	114	82	138	211	53	150	31	56	106	111	78
Cr	82.1	75.3	21	82	109	21	123	41	< 13.7	61.6	34.2	27.4	102.6	21	34.2	41.1	21	20.5	14	95.8	54.7	171.1
Ni	49.1	45	17.5	42.4	55.7	17	50.8	18	13.9	28.3	13.3	15.6	43.5	13.1	16.6	22.2	10.2	18.2	3.9	38.9	27.6	49
F	1860	1790	1850	1620	1780	1810	1190	2060	1850	1160	1820	2200	2750	1510	2750	740	1660	210	300	950	1580	1660

[a] Finnish national coorninates.
[b] Dr, diorite; Gr, granite; Hy, hybrid.
[c] Mg#, magnesium number (calculated by SINCLAS (Verma et al. 2002)).

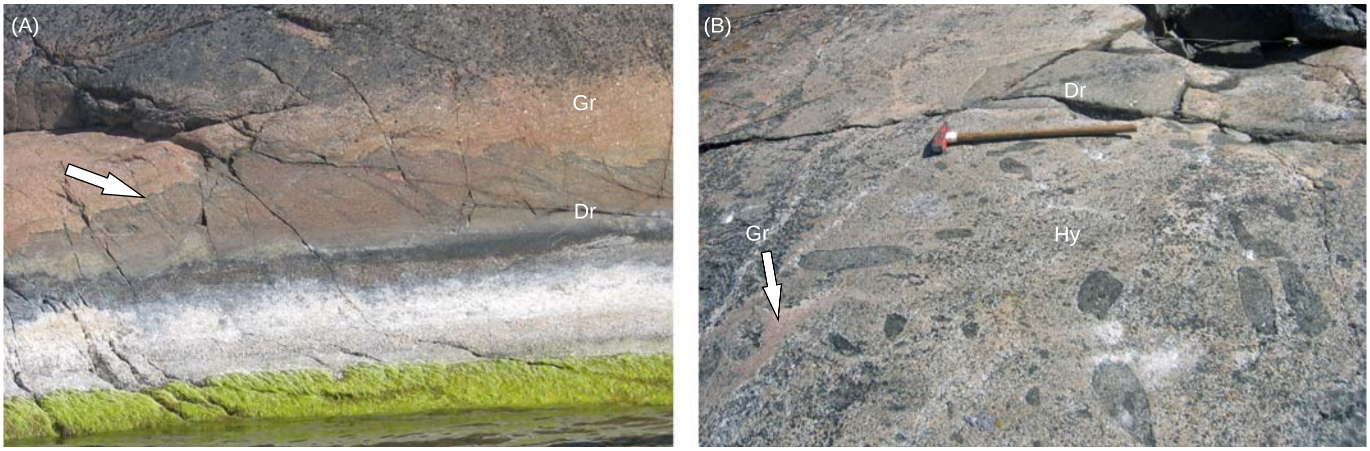

Fig. 2. **A**. Subhorizontal wavy contact between Korpo diorite (Dr, below) and granite (Gr, on top) observed on a subvertical cliff at the shoreline on the island of Dimanskär. Contact is indicated by an arrow. The width of the view is c. 2 m. **B**. Diorite and granite mixture forming a hybrid. The hammer is ~60 cm long. Dr, diorite; Gr, granite; Hy, hybrid.

background, laser-induced elemental fractionation, mass discrimination and drift in ion counter gains and reduced to U–Pb isotope ratios by calibration to concordant reference zircons of known age, using protocols adapted from Andersen et al. (2004) and Jackson et al. (2004). Standard zircons GJ-01 (609 ± 1 Ma; Belousova et al. 2006) and an in-house standard A382 (Patchett & Kouvo 1986; 1877 ± 2 Ma by SIMS and from recent concordant analysis by thermal ionization mass spectrometer (TIMS)) were used for calibration. The calculations were done off-line, using an interactive spreadsheet program written in Microsoft Excel/VBA by T. Andersen (Rosa et al. 2009). To minimize the effects of laser-induced elemental fractionation, the depth-to-diameter ratio of the ablation pit was kept low, and isotopically homogeneous segments of the time-resolved traces were calibrated against the corresponding time interval for each mass in the reference zircon. To compensate for drift in instrument sensitivity and Faraday versus electron multiplier gain during an analytical session, a correlation of signal versus time was assumed for the reference zircons. A description of the algorithms used is provided in Rosa et al. (2009).

The isotope data were calculated and plotted using the Isoplot software (Ludwig 2003). The results of the analyses are shown in Table 1.

Twenty-two whole-rock samples were analysed at Acme Analytical Laboratories Ltd. (Acme) in Vancouver, Canada. The samples were pulverized in a mild steel swingmill and after $LiBO_2$ fusion and HNO_3 dilution, the major elements and Cr were analysed by ICP-ES. The other trace elements were analysed by ICP-MS. F was analysed by assay method. The geochemical data were plotted using the GCDkit software (Janoušek et al. 2006). The results of the analyses are shown in Table 2.

Results

U–Pb zircon dating

The zircon crystals from the *Rauma diorite* sample (from Rauma city) are of variable shape and size, but the majority are euhedral to subhedral in shape and 100–300 μm in length, with the longest crystals being up to 500 μm in length. All the zircons are internally quite homogeneous and zoning is only occasionally observed. Separate core domains are not obvious in the BSE images either. Some crystals show narrow metamict alteration areas along outer rims and cracks, which are common in nearly all crystals (Fig. 3A, B). Thirty-two spots, each from a different zircon crystal, were analysed. The measurements yielded a concordia age of 1865 ± 9 Ma (mean square weighted deviation (MSWD) = 0.26; Fig. 4A).

The zircons from the *Korpo diorite* sample (from Galtby) are clearly of two different morphologies: rounded (Fig. 3C) and prismatic (Fig. 3D). The rounded zircons are in general 100–200 μm in diameter and commonly show internal zonation. The prismatic zircons, including stubby crystals, are 100–400 μm in length and form the majority of the zircons. Many of these also show zoning. Twenty-nine spots, each on a different zircon crystal, were analysed. The analyses revealed no age differences between the different zircon types. Omitting two analyses with large errors, the sample yielded a concordia age of 1852 ± 4 Ma (MSWD = 0.78; Fig. 4B).

The *Korpo granite* sample (from Dimanskär) has a variety of zircon morphologies including small rounded (< 100 μm) and prismatic 100–200 μm long crystals. The majority of the zircons are metamict and altered to some extent. Many crystals show inner domains, occasionally zoned and outer rims separated by metamict areas (Figs. 3E, F). Twenty-eight spots on sixteen different zircon crystals were analysed. The analyses revealed, based on $^{207}Pb/^{206}Pb$ ages, one Archaean, c. 2.6 Ga core age and one older Palaeoproterozoic, c. 1.91 Ga age, which probably also was inherited. Four analyses were discordant (one reversely) and two showed unrealistically young ages of unknown reason (Fig. 4C; Table 1). The remaining 16 concordant analyses yielded a concordia age of 1849 ± 8 Ma (MSWD = 13; Fig. 4D). Only a few rim domains were wide enough to be analysed by a 25 μm laser spot. Five analyses were done at the rim domains, one of which was discordant. They yielded a concordia age of 1827 ± 14 Ma ($n = 4$; MSWD = 10.7) or, including the discordant analysis, an upper intercept age of 1822 ± 16 Ma ($n = 5$; MSWD = 0.17) and a weighted average $^{207}Pb/^{206}Pb$ age of 1822 ± 12 Ma ($n = 5$; MSWD = 0.15; Fig. 4E).

Geochemistry

Major elements. – The mafic rocks from Rauma, Olkiluoto and Korpo show quite variable geochemical characteristics. The SiO_2 contents range between 47 and 60 wt% and compositions

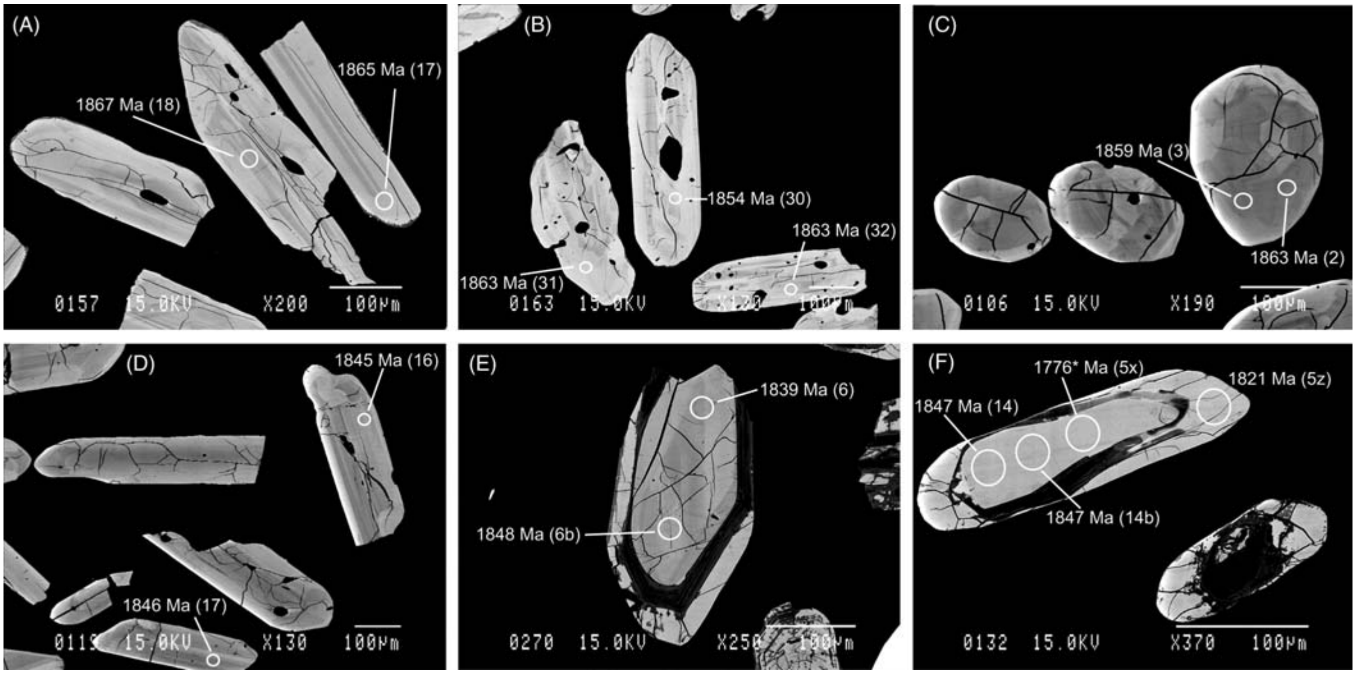

Fig. 3. BSE images of selected zircons. **A**, **B** are from the Rauma diorite, **C**, **D** are from the Korpo diorite and **E**, **F** are from the Korpo granite. The spot sizes (25 μm) are indicated by circles. Ages refer to $^{207}Pb/^{206}Pb$ ages followed by the analysis code (in brackets). Refer to Table 1 for more details. Ages indicated by * were not used in the age calculations.

straddle the fields of diorites, gabbros, monzogabbros and monzodiorites in the total alkali versus SiO_2 (TAS) diagram (Fig. 5). For simplicity, we call all these rocks diorites in accordance with field descriptions used during sampling. Compared to synorogenic magmas, most of the diorites show elevated Fe_2O_3, P_2O_5 and TiO_2 contents (Fig. 6A–C) and plot in the high-K calc-alkaline and shoshonitic fields in the K_2O versus SiO_2 diagram (Fig. 6D). Also, the K_2O/Na_2O ratios >0.5 point towards a shoshonitic affinity (Turner et al. 1996; Fig. 6E). Apart from the three slightly peraluminous samples, the rocks are metaluminious (Fig. 6F). Compared to the synorogenic 1872 ± 3 Ma Uusikaupunki diorite and the post-collisional 1815 ± 2 Ma Turku monzodiorite, the compositions show more similarities with the post-collisional rocks apart from the fact that at corresponding SiO_2 concentrations the Fe_2O_3, P_2O_5 and TiO_2 contents are even higher in the post-collisional magmas. The synorogenic rocks have lower contents regarding these elements but are higher in SiO_2 and MgO (Fig. 6G). The diorite samples show lower Mg contents than the 1.97 synorogenic rocks. The Korpo samples have the lowest Mg contents of the group similar to the 1.815 Ga post-collisional rocks (Fig. 6H).

The Korpo granite is a garnet-bearing, peraluminous rock which is high in SiO_2 and K_2O and with high K_2O/Na_2O ratios but low concentrations of Fe_2O_3, MgO and TiO_2 (Fig. 6). Geochemically the granite is similar to those described as "late Svecofennian granites of southern Finland", i.e. products of crustal melting (e.g. Huhma 1986; Suominen 1991; Ehlers et al. 1993; Lahtinen 1996; Johannes et al. 2003).

Those samples that, based on field evidence, were interpreted as hybrids between the Korpo diorite and granite generally plot between the diorite and granite samples in almost all cases in Figs. 6 and 7.

Trace elements. – Selected trace element diagrams (Fig. 7) in most cases show the same relationships as the major element diagrams, i.e. the compositions of the diorites are heterogenous but in many aspects intermediate between those of the older synorogenic rocks and the younger post-collisional rocks at the same SiO_2 level. This is true at least for Ba (c. 500–1000 ppm; Fig. 7A), F (c. 1000–2000 ppm; Fig. 7B) and Zr (c. 200–400 ppm; Fig. 7C), but Sr contents (c. 500–1500 ppm) are clearly higher in the post-collisional rocks (Fig. 7D), and are even higher in other post-collisional intrusions in southern Finland (Rutanen et al. 2011). Contents of Nb and Rb are on the same levels as the post-collisional rocks (Fig. 7E,F).

The chondrite-normalized rare earth element diagrams and the primitive mantle-normalized multi-element diagrams (Fig. 8) show the fractionated nature of the magmas and high concentrations of the light rare earth elements (LREEs) and large ion lithophile elements (LILEs). However, concentrations of these elements are even higher in the post-collisional rocks. The Korpo diorite has negative anomalies for Eu and Sr, probably because of plagioclase fractionation, and all diorites except one Korpo sample have negative Nb and Ti anomalies in the multi-element diagrams.

The most striking trace element feature of the granites is their low HREE and Y contents. These are also partly seen in the hybrids.

Discussion

Age data

The Svecofennian accretionary stage ceased at c. 1.87 Ga. It was followed by uplift resulting in weathering and erosion of the uppermost parts of the crust formed during the Fennian orogeny as shown by the lateritic sediments associated with mature

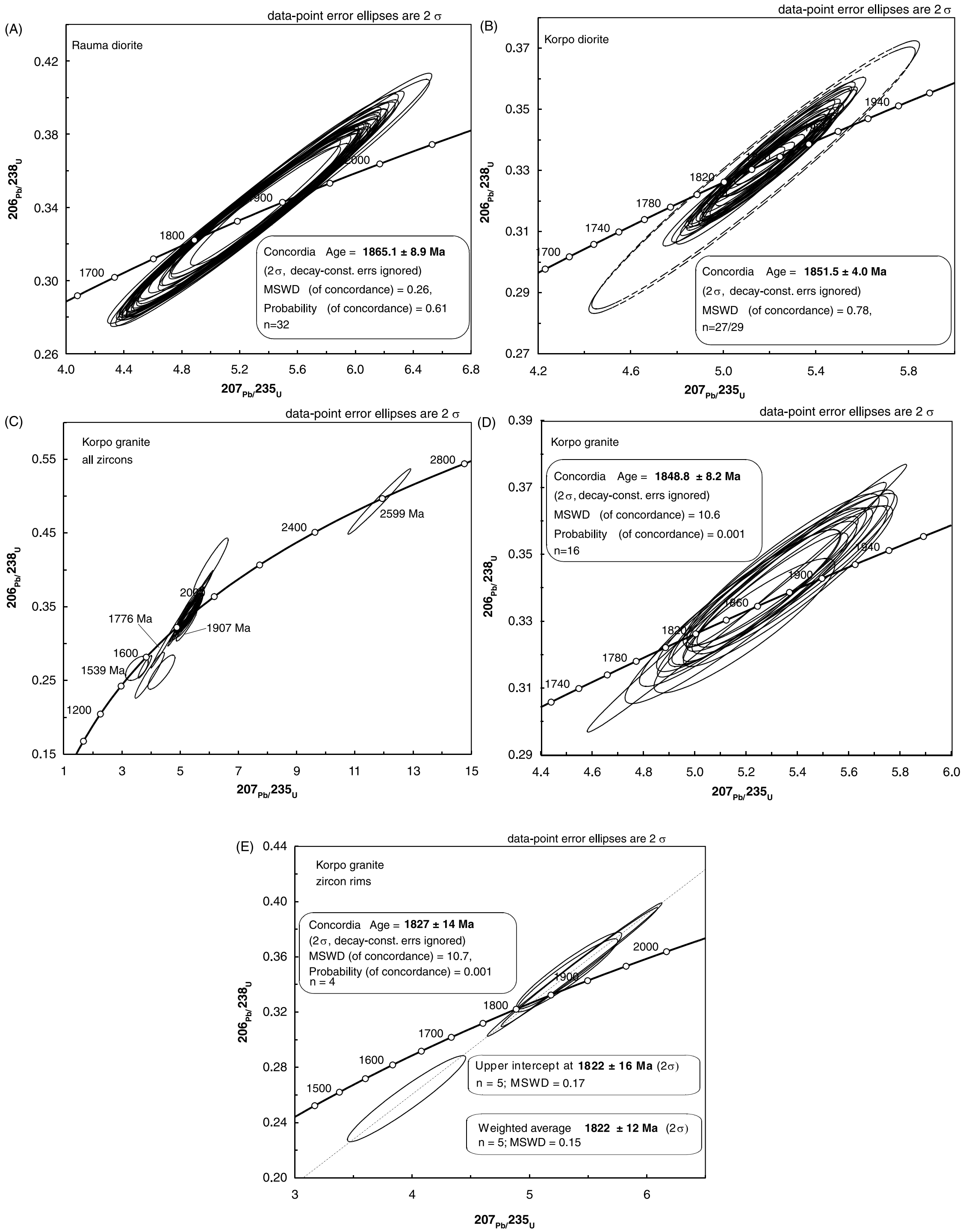

Fig. 4. **A** Concordia diagrams for the LA-MC-ICP-MS analyses on zircons from the Rauma diorite, **B** the Korpo diorite and **C**–**E** the Korpo granite. In the Korpo diorite sample (**B**) the two analyses excluded from the age calculation are shown with dashed lines. **C** shows all analyses done on the granite sample. The two oldest (inherited) and two younger concordant $^{207}Pb/^{206}Pb$ ages, which were not used in the age calculations, are reported next to the error ellipses. The data clusters in **C** are enlarged in **D** and **E**.

quartzites. The youngest material in these sediments is derived from the underlying Fennian bedrock (Lahtinen & Nironen 2010; Nironen 2011; Nironen & Mänttäri 2012). This indicates that the Svecofennian orogen consists of separate phases interrupted by an intra-orogenic stage as previously suggested by Lahtinen et al. (2002, 2005) and Bergman et al. (2008). The well-defined 1852 ± 4 Ma age of the Korpo diorite is c. 20 million years (m.y.) younger than the synorogenic diorites of south-west Finland (Patchett & Kouvo 1986; Väisänen et al. 2012), but the rock intruded prior to the Svecobaltic continent–continent collision stage, which demonstrates that the mafic magmatism described in this study belongs to the proposed

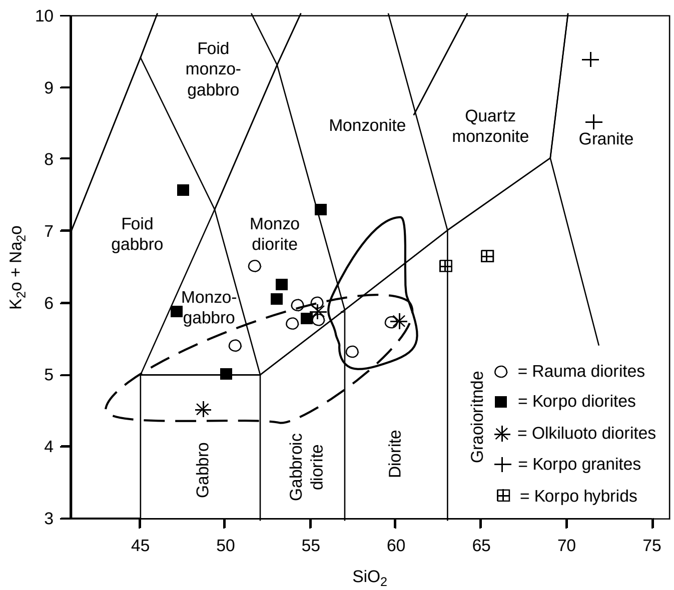

Fig. 5. TAS diagram after Middlemost (1994). The field delimited by a solid line indicates the compositions of the synorogenic 1872 ± 3 Ma Uusikaupunki diorites (Väisänen et al. 2012) and the one by a dashed line indicates those of the post-collisional 1815 ± 2 Ma Turku monzodiorites (Väisänen et al. 2000).

intra-orogenic stage. Combined with similar age data from Olkiluoto (1863–1851 Ma), it is evident that the intra-orogenic stage comprises both mantle- and crustal-derived magmatism.

Within errors, the 1863 ± 6 Ma intrusion in Olkiluoto (Mänttäri et al. 2006) and the 1865 ± 9 Ma intrusion in Rauma (this study) may be synorogenic. However, from a geochemical point of view (Figs. 6, 7), these rocks are more similar to those in Korpo. Therefore, we suggest that the geochemical transition from synorogenic to intra-orogenic magma types took place around 1.865 Ga.

Recent single zircon age data indicate that there was no long-lasting gap in mantle-derived magmatism in the Svecofennian orogen in southern Finland. The synorogenic c. 1.87 Ga stage was closely followed by c. 1.86–1.84 Ga mafic magmatism (Mänttäri et al. 2006, 2007; Pajunen et al. 2008; this study) that basically defines the intra-orogenic stage. Considering that single zircon dating methods have been used only for about 10 years, it is probable that future studies will discover more rocks within this time-span (e.g. Nevalainen et al. 2011). Pajunen et al. (2008) presented a SIMS age of 1838 ± 4 Ma for the Jyskelä gabbro (Fig. 1B). To date, that is the lowest obtained age for mafic magmatism in southern Finland before the so-called post-collisional magmatic stage that started at 1815 ± 2 Ma (Rutanen et al. 2011 and references therein).

The Korpo diorite is associated with a large volume of anatectic granites. The contact relationships and occurrence of hybrids indicate simultaneous mafic and felsic magmatism (Fig. 2). The 1849 ± 8 Ma age of the granite is, within errors, coeval with that of the diorite, and consistent with the idea that the mafic magmas provided heat for crustal melting that produced the granites. Within the same zone of granites, but farther east, a similar granite occurs in form of the flat-lying Perniö granite sheet (Selonen et al. 1996; Fig. 1B). The single zircon ages obtained for the Perniö granite are 1835 ± 12 Ma (Kurhila et al. 2005) and 1853 ± 18 Ma (Kurhila et al. 2010), which indicates that the Korpo granite may represent a western variety of the Perniö granite. Situated even further to the east, the Västankvarn granite (Fig. 1B), dated by Skyttä & Mänttäri (2008) at 1843 ± 3 Ma (concordia age) and 1846 ± 6 Ma (upper intercept age), also intruded within the same time frame.

From this discussion it is apparent that between c. 1.865 and 1.84 Ga, considerable volumes of magma were intruded into the middle crust during the intra-orogenic stage. At the present surface, the mafic rocks are subordinate, whereas the granites are one of the main rock types in this part of the Svecofennian orogen.

The rim domains of the zircons from the Korpo granite yielded a concordia age of 1827 ± 14 Ma, an upper intercept age of 1822 ± 16 Ma and a weighted average age of 1822 ± 12 Ma. This age most likely reflects a metamorphic overprint since it is in accordance with well-defined metamorphic ages within the nearby areas. The age has rather large errors, but combined with the more precise 1824 ± 5 Ma zircon age from the Turku area (Väisänen et al. 2002), the 1824 ± 5 Ma monazite age from the Kemiö area (Levin et al. 2005), the 1830–1815 Ma monazite ages from the West Uusimaa area (Mouri et al. 2005) and the 1815 ± 3 Ma zircon age from the Orijärvi area (Väisänen & Kirkland 2008), the data presented in this study suggest that the age of peak metamorphism spans over c. 1.83–1.81 Ga also in the Korpo area. They also verify that the intra-orogenic magmatism in Korpo pre-dated the regional high-grade metamorphism. Similar age relationships have also been found in the Ljusdal Domain in central Sweden, where magmatism and related contact metamorphism occurred at c. 1.86–1.84 Ga and peak metamorphism at 1.83–1.82 Ga (Högdahl et al. 2012).

Geochemical data

The compositions of the intra-orogenic 1865–1852 Ma mafic magmatic rocks are in most cases intermediate between the earlier synorogenic and the later post-collisional magmatism. Concentrations of many elements are, however, closer to those of the post-collisional rocks. This suggests that they derive from the same or similar source regions and conditions. The varying, but in general, moderate Mg contents (Fig. 6H) and Ni contents (Fig. 7G) suggest that the magmas are not primary melts, but fractionated olivine during ascent. The negative Sr and Eu anomalies in the Korpo trace element patterns indicate plagioclase fractionation.

The trace element ratios of Zr/Hf are higher than the chondritic value of 36 (Fig. 9). This has been interpreted as a sign of carbonate metasomatism within the mantle (Dupuy et al. 1992). The enriched compositions of the post-collisional rocks have been interpreted similarly and subduction-induced carbonate metasomatism has been proposed (Eklund et al. 1998; Andersson et al. 2006a; Woodard 2010). The same model can be applied to the intra-orogenic magmas in this study, and it is likely that source enrichments of LREEs, LILEs, F and P_2O_5 are related to similar processes. The negative Nb, Zr and Ti anomalies in the primitive mantle-normalized multi-element diagrams (Fig. 8) also indicate a subduction component from an earlier subduction history (cf. Rutanen et al. 2011 and references therein).

Compositions of anatectic granites in southern Finland vary as a function of their sources. The granites are typically of S-type and derived from metasedimentary rocks (Lahtinen 1996; Johannes et al. 2003). In contrast, Kurhila et al. (2010) interpreted that the Perniö granite (Fig. 1) was derived from an older metaigneous source. The same also probably pertains to the Korpo granite, as the A/CNK index below 1.1 is too low for

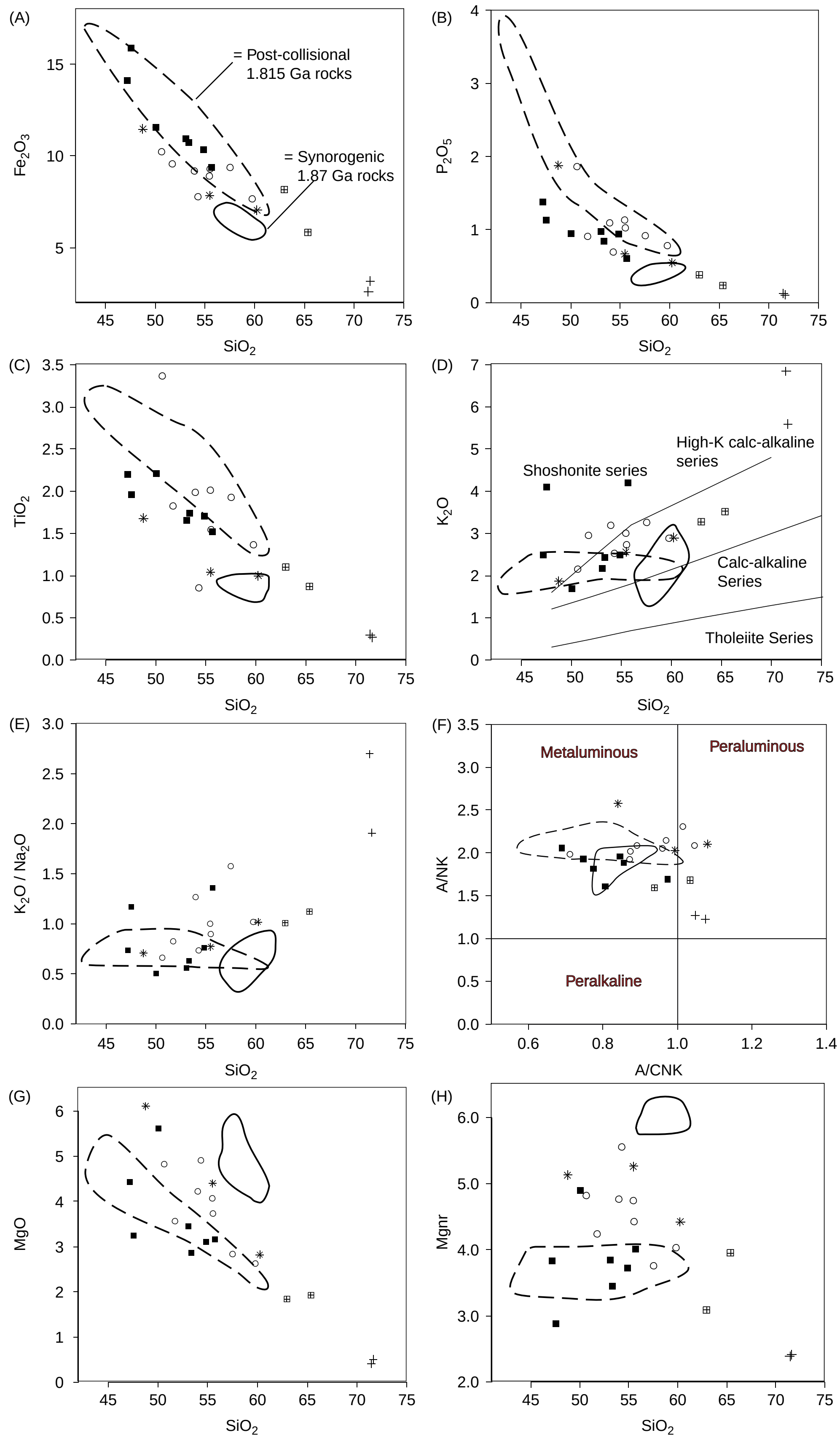

Fig. 6. Selected major elements versus SiO_2, major element ratios versus SiO_2 and A/NK versus A/CNK diagrams. The field for post-collisional rocks is based on data in Väisänen et al. (2000) and the field for synorogenic rocks is based on data in Väisänen et al. (2012). Field boundaries in **D** are according to Peccerillo & Taylor (1976). Symbols are as in Fig. 5.

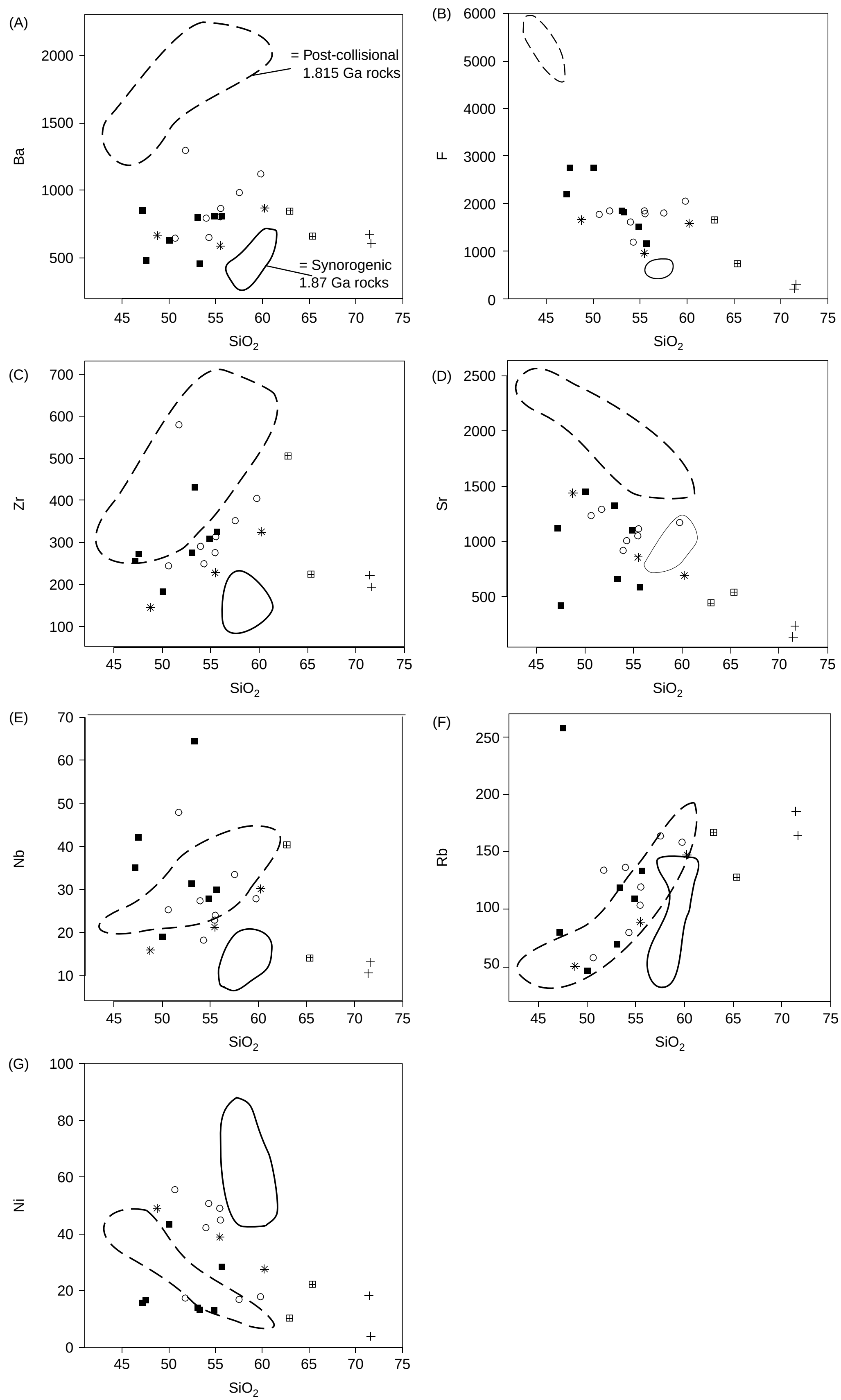

Fig. 7. Selected trace elements versus SiO_2 diagrams. The field for post-collisional rocks is based on data in Väisänen et al. (2000) and the field for synorogenic rocks is based on data in Väisänen et al. (2012). Symbols are as in Fig. 5.

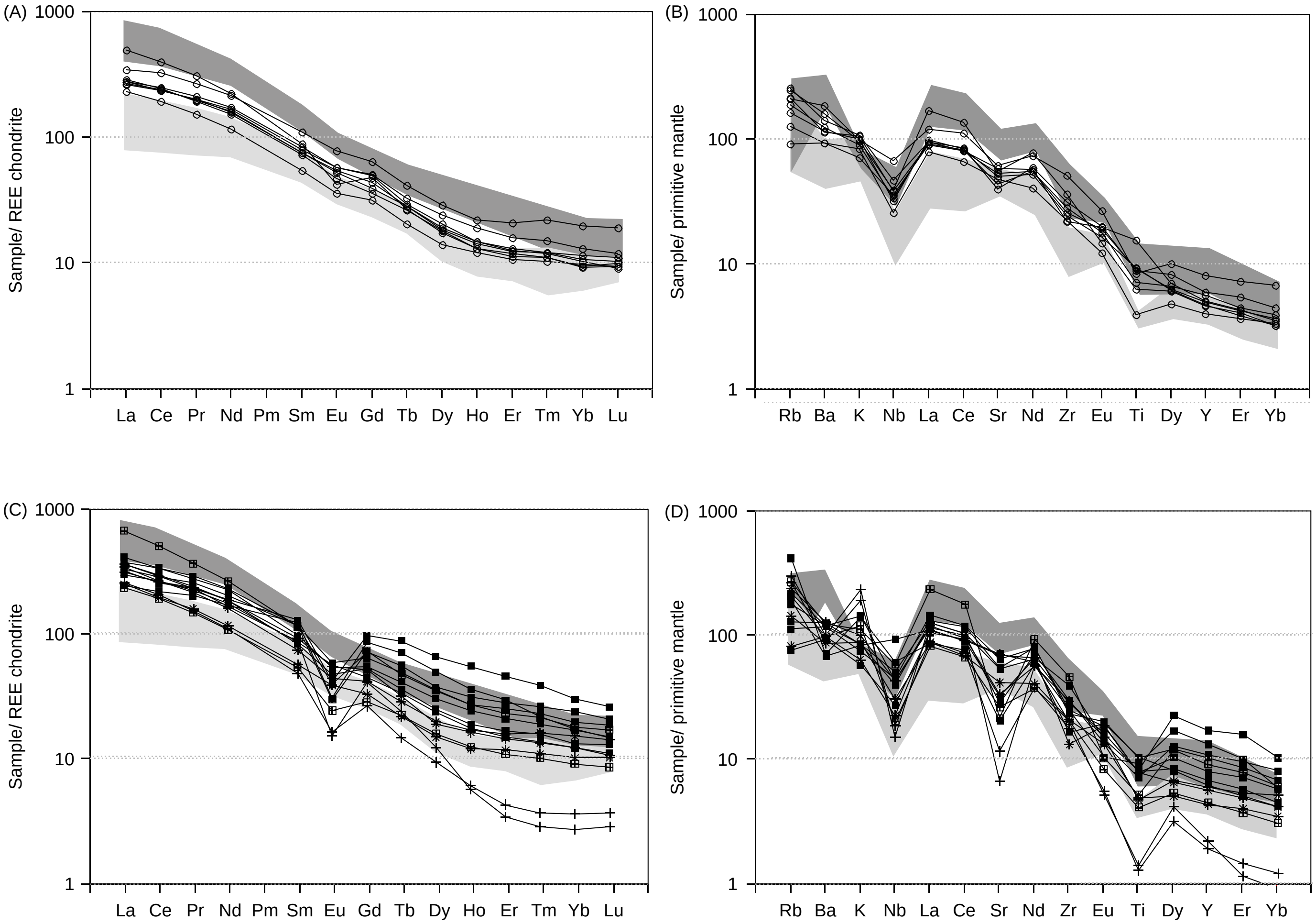

Fig. 8. Chondrite-normalized REE diagrams (**A**, **C**) and primitive mantle-normalized multielement diagrams (**B**, **D**). Dark grey fields denote the range of compositions of the post-collisional 1815 ± 2 Ma Turku monzodiorites (Väisänen et al. 2000) and the light grey fields the compositions of the synorogenic 1872 ± 3 Ma Uusikaupunki diorites (Väisänen et al. 2012). Normalization values are after Sun & McDonough (1989). **A** and **B** contain samples from Rauma and **C** and **D** contain the other samples. Symbols are as in Fig. 5.

an S-type granite (Fig. 6F; Chappell & White 2001) and as low HREE contents are a common feature of the synorogenic felsic intrusive rocks in south-west Finland (Väisänen et al. 2012). On the other hand, the inherited 2.6 Ga zircons point to at least some sedimentary component in the source. Taken together, the evidence points to a mixed source (cf. Kurhila et al. 2011).

Thermal implications

SS was characterized by high heat flow during the late (Svecobaltic) stage of the Svecofennian orogeny. Peak metamorphism is generally regarded to have taken place between c. 1.83 and 1.81 Ga (Korsman et al. 1999; Väisänen et al. 2002; Mouri et al. 2005; Andersson et al. 2006b; Högdahl et al. 2008; Mänttäri et al. 2010; this study), but locally as late as c. 1.795 Ga (Andersson et al. 2006b; Baltybaev et al. 2006; Väisänen & Kirkland 2008). However, recent data indicate that the high grade metamorphism actually started earlier based on the metamorphic zircons dated at c. 1.85–1.84 Ga (Torvela et al. 2008; Högdahl et al. 2012; Väisänen et al. 2012). The increasing number of anatectic granites of the same age interval also indicates that high heat flow began already at c. 1.85 Ga (Kurhila et al. 2005; Skyttä & Mänttäri 2008; Kurhila et al. 2010). It is noteworthy that the 1.86–1.84 Ga magmatism is common also in central Sweden (Högdahl et al. 2008).

The heat source for the high grade late Svecofennian metamorphism has been the subject of much speculation. Korsman (1977) stated that heat was provided by crustal thickening. This idea was expanded by Kukkonen & Lauri (2009) who proposed that crustal thickening and magmatism at c. 1.87–1.86 Ga were followed by radioactive decay that provided heat for later metamorphism. Schreurs & Westra (1986) proposed that, based on the existence of a gravity anomaly within the West Uusimaa area, a large amount of mafic magma was intruded into the middle crust beneath the area where granulite facies metamorphism occurred and that magmatism, assisted by CO_2 fluxing, provided the heat for metamorphism. In the Turku area, charnockites were considered as a heat source by Van Duin (1992), and Väisänen et al. (2000) proposed that shoshonitic mantle-derived intrusions in the Turku granulite area were a heat source for metamorphism. The latest models from the West Uusimaa granulite area emphasize the role of extensional tectonism (Nironen et al. 2006; Skyttä & Mänttäri 2008). None of these models can unequivocally account for the long duration of metamorphism, from c. 1.85 to c. 1.795 Ga, i.e. spanning c. 20–70 m.y. after the accretionary stage.

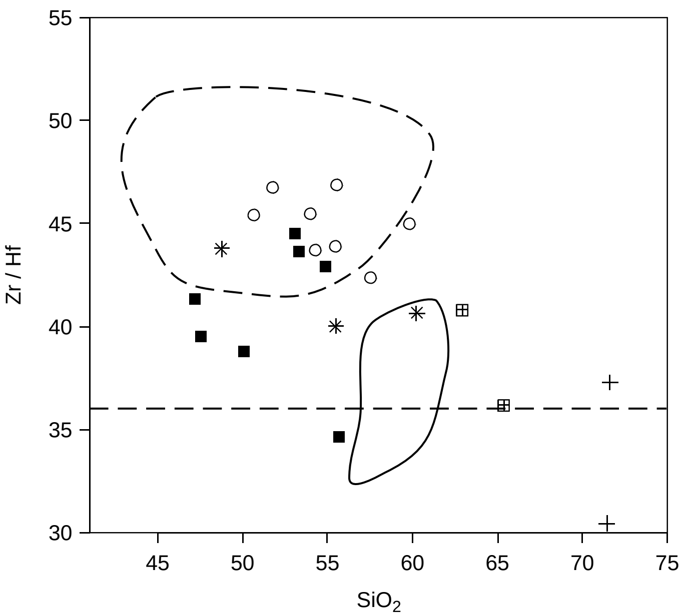

Fig. 9. Zr/Hf versus SiO_2 diagram. The chondritic value of 36 (Sun & McDonough 1989) is indicated by the dashed line. Fields and symbols are as in Figs. 5, 6 and 7.

It is now evident that 1.865–1.84 Ga mantle-derived magmatism was quite common in southern Finland, and that there were no long-term gaps in mantle-derived magmatism and heat input. This suggests that the mafic magmatism might have been an important heat source. As the structures and the associated magmatic intrusions prior to the continent-continent collision were subhorizontal (e.g. Ehlers et al. 1993; Selonen & Ehlers 1998; Skyttä et al. 2006; Skyttä & Mänttäri 2008), the Rauma and Korpo diorites also probably intruded as subhorizontal sheets with thicknesses in excess of 500 m. These must have had a wide-spread and substantial thermal impact as directly indicated by the large amount of basically coeval anatectic granites around the Korpo diorite bodies. The geological map of the Rauma area also shows large amounts of granites in the area (Suominen & Torssonen 1993), as would be expected by the model if expanded into this area.

Harley (1992) pointed out that crustal thickening alone cannot explain the regional high grade metamorphism in Proterozoic orogens. Some heat source, external to the crust, is also needed. Accordingly, we agree with the model of Schreurs & Westra (1986) in which it is the heat input from the mantle, in the form of mafic magmas, which primarily was responsible for the high heat flow in southern Finland. Crustal temperatures had reached amphibolite facies temperatures already during the accretional stage at c. 1.87 Ga and rose during and after the 1.86–1.84 Ga intra-orogenic magmatic stage. Maximum high temperature–low pressure granulite facies conditions were reached at c. 1.83–1.81 Ga during the continental collision, i.e. c. 10–30 m.y. later than the youngest known intra-orogenic intrusions. This indicates that evidence of mafic magmatism of that age interval (or slightly older) remains to be found unless it is hidden below the present erosional level. We acknowledge that radioactive decay, as in the model of Kukkonen & Lauri (2009), may have had an important role in the thermal budget of the crust and it is possible that no additional mafic magma intrusions were needed to reach granulite facies temperatures during peak metamorphism.

Tectonic setting

The tectonic setting of the intra-orogenic stage is a matter of debate. In the tectonic model of Lahtinen et al. (2005), the time interval 1.87–1.85 Ga was inferred to be a large-scale orogenic collapse of the overthickened Fennian orogen while the crust was still hot (c.f. Korja et al. 2009). The lithospheric thinning would lead to upwelling of the asthenosphere, thinning of the crust and rising temperatures in the lower and middle crust, subsequently leading to formation of granites and migmatites. Lahtinen & Nironen (2010) discussed the tectonic setting of the intra-orogenic stage and also suggested back-arc spreading related to an outboard subduction zone in the south-west or intra-continental rifting as alternative reasons for extension. On the other hand, Hermansson et al. (2008) and Saalmann et al. (2009) consider that a retreating subduction zone caused alternating compressional and extensional stages. Whatever the ultimate drive for the tectonism was, the models imply that some sort of extensional period prevailed as indicated by the sedimentary basins filled with quartzites (Bergman et al. 2008; Lahtinen & Nironen 2010; Nironen & Mänttäri 2012).

The coeval sedimentation on the surface and plutonism at deeper levels are anticipated in the model above. In south-east Finland, where remnants of the intra-orogenic supracrustal rocks are preserved (Fig. 1B), no contemporaneous intrusions are encountered (Lahtinen & Nironen 2010). Our single zircon data from south-west Finland unambiguously verify that, indeed, voluminous mantle- and crust-derived intra-orogenic magmas intruded into the middle crust, but there are no coeval sediments. This indicates that these two areas (Fig. 1B) were at different crustal levels at 1.87–1.85 Ga. Korja et al. (2009) and Lahtinen & Nironen (2010) suggested that, during the intra-orogenic stage, the upper and middle crust were detached from each other: rift basins formed in the uppermost crust while horizontal ductile flow and vertical shortening combined with magmatic activity took place in the middle and lower crust. This is what we see in our examples; intra-orogenic magmas originally intruded as subhorizontal sheets (e.g. Ehlers et al. 1993) that were only later folded into steeper structures.

It remains unclear when the sedimentary and magmatic areas were brought together to their present crustal level. Either they were folded and/or thrusted during the Svecobaltic shortening at 1.84–1.81 Ga (Lahtinen & Nironen 2010) or moved to different levels in later extensional faulting postdating the Svecobaltic orogeny at 1.79–1.77 Ga (Väisänen & Skyttä 2007). Combinations of the two models are also possible.

Conclusions

1. A voluminous "intra-orogenic" magmatic event between c. 1865 and 1840 Ma is well recorded in Southern Svecofennia. Consequently, there are no long-lasting time gaps in magmatism during the Svecofennian orogeny in southern Finland and, more importantly, no prompt termination of mantle-derived magmatism at 1.87 Ga.
2. The intra-orogenic magmatism comprises both mantle and crustal components. The mantle-derived intrusions formed during a prolonged period and consist of high-K and shoshonitic mafic magmas enriched in Fe, Ti, P and F, as well as LILEs and LREEs. The enrichment level is intermediate

between those of the older synorogenic and younger post-collisional mafic magmas. The enrichment reflects previous subduction-related mantle metasomatism. The crustal-derived anatectic granites, accordingly, show a similarly wide age range.

3. The intra-orogenic magmatism assisted by heat from radioactive decay has been the main source of the high heat flow at c. 1.85–1.81 Ga in the southern Svecofennian terrane of Finland.

Acknowledgements. — Jussi Mattila from Posiva Oy is thanked for his help at Olkiluoto. Arto Peltola made the zircon mounts and thin sections. The comments by two anonymous reviewers and editor Magnus Ripa greatly helped to improve the manuscript. This study was funded by the Academy of Finland (project 117311) and the Otto A. Malm Foundation. This is a Finland Isotope Geosciences Laboratory (SIGL) contribution.

References

Andersen, T., Griffin, W.L., Jackson, S.E., Knudsen, T.-L. & Pearson, N.J., 2004: Mid-proterozoic magmatic arc evolution at the southwest margin of the Baltic Shield. *Lithos 73*, 289–318.

Andersson, U.B., Eklund, O., Fröjdö, S. & Konopelko, D., 2006a: 1.8 Ga magmatism in the Fennoscandian shield; lateral variations in subcontinental mantle enrichment. *Lithos 86*, 110–136.

Andersson, U.B., Högdahl, K., Sjöström, H. & Bergman, S., 2006b: Multistage growth and reworking of the Palaeoproterozoic crust in the Bergslagen area, southern Sweden: Evidence from U–Pb geochronology. *Geological Magazine 143*, 679–697.

Baltybaev, S.K., Levchenkov, O.A., Levsky, L.K., Eklund, O. & Kilpeläinen, T., 2006: Two metamorphic stages in the Svecofennian domain: Evidence from the isotopic geochronological study of the Ladoga and Sulkava metamorphic complexes. *Petrology 14*, 247–261.

Belousova, E.A., Griffin, W.L. & O'Reilly, S.Y., 2006: Zircon crystal morphology, trace element signatures and Hf isotope composition as a tool for petrogenetic modeling: Examples from Eastern Australian granitoids. *Journal of Petrology 47*, 329–353.

Bergman, S., Högdahl, K., Nironen, M., Ogenhall, E., Sjöström, H., Lundqvist, L. & Lahtinen, R., 2008: Timing of Palaeoproterozoic intra-orogenic sedimentation in the central Fennoscandian Shield: Evidence from detrital zircon in metasandstone. *Precambrian Research 161*, 231–249.

Cagnard, F., Gapais, D. & Barbey, P., 2007: Collision tectonics involving juvenile crust: The example of the southern Finnish Svecofennides. *Precambrian Research 154*, 125–141.

Chappell, B.W. & White, A.J.R., 2001: Two contrasting granite types: 25 years later. *Australian Journal of Earth Sciences 48*, 489–499.

Chardon, D., Gapais, D. & Cagnard, F., 2009: Flow of ultra-hot orogens: A view from the Precambrian, clues for the Phanerozoic. *Tectonophysics 477*, 105–118.

Dupuy, C., Liotard, J.M. & Dostal, J., 1992: Zr/Hf fractionation in intraplate basaltic rocks: Carbonate metasomatism in the mantle source. *Geochimica et Cosmochimica Acta 56*, 2417–2423.

Edelman, N., 1973: Nagu. Geological map of Finland 1:100 000: Pre-quaternary rocks, sheet 1034, Geological Survey of Finland, Espoo.

Ehlers, C., Lindroos, A. & Selonen, O., 1993: The late Svecofennian granite-migmatite zone of southern Finland-a belt of transpressive deformation and granite emplacement. *Precambrian Research 64*, 295–309.

Ehlers, C., Skiöld, T. & Vaasjoki, M., 2004: Timing of Svecofennian crustal growth and collisional tectonics in Åland, SW Finland. *Bulletin of the Geological Society of Finland 76*, 63–91.

Eklund, O., Konopelko, D., Rutanen, H., Fröjdö, S. & Shebanov, A.D., 1998: 1.8 Ga Svecofennian post-collisional shoshonitic magmatism in the Fennoscandian shield. *Lithos 45*, 87–109.

Gorbatschev, R. & Bogdanova, S., 1993: Frontiers in the baltic shield. *Precambrian Research 64*, 3–21.

Harley, S., 1992: Proterozoic granulite areas. *In* K.C. Condie (ed.): *Proterozoic crustal evolution*, 301–359. Elsevier.

Hermansson, T., Stephens, M.B., Corfu, F., Page, L.M. & Andersson, J., 2008: Migratory tectonic switching, western Svecofennian orogen, central Sweden: Constraints from U/Pb zircon and titanite geochronology. *Precambrian Research 161*, 250–278.

Högdahl, K., Majka, J., Sjöström, H., Persson Nilsson, K., Claesson, S. & Konečný, P., 2012: Reactive monazite and robust zircon growth in diatexites and leucogranites from a hot, slowly cooled orogen: Implications for the Palaeoproterozoic tectonic evolution of the central Fennoscandian Shield, Sweden. *Contributions to Mineralogy and Petrology 163*, 167–188.

Högdahl, K. & Sjöström, H., 2001: Evidence for 1.82 Ga transpressive shearing in a 1.85 Ga granitoid in central Sweden: Implications for the regional evolution. *Precambrian Research 105*, 37–56.

Högdahl, K., Sjöström, H., Andersson, U.B. & Ahl, M., 2008: Continental margin magmatism and migmatisation in the west-central Fennoscandian Shield. *Lithos 102*, 435–459.

Högdahl, K., Sjöström, H. & Bergman, S., 2009: Ductile shear zones related to crustal shortening and domain boundary evolution in the central Fennoscandian Shield. *Tectonics 28* (*TC1003*), 18 pp, DOI: 10.1029/2008TC002277.

Horstwood, M.S.A., Foster, G.L., Parrish, R.R., Noble, S.R. & Nowell, G.M., 2003: Common-Pb corrected *in situ* U–Pb accessory mineral geochronology by LA-MC-ICPMS. *Journal of Analytical Atomic Spectrometry 18*, 837–846.

Huhma, H., 1986: Sm–Nd, U–Pb and Pb–Pb isotopic evidence for the origin of the Early Proterozoic Svecokarelian crust in Finland. *Geological Survey of Finland, Bulletin 337*, 48 pp.

Jackson, S.E., Pearson, N.J., Griffin, W.L. & Belousova, E.A., 2004: The application of laser ablation-inductively coupled plasma-mass spectrometry to *in-situ* U–Pb zircon geochronology. *Chemical Geology 211*, 47–69.

Janoušek, V., Farrow, G. & Erban, V., 2006: Interpretation of whole-rock geochemical data in igneous geochemistry: Introducing Geochemical Data Toolkit (GCDkit). *Journal of Petrology 47*, 1255–1259.

Johannes, W., Ehlers, C., Kriegsman, L.M. & Mengel, K., 2003: The link between migmatites and S-type granites in the Turku area, southern Finland. *Lithos 68*, 69–90.

Kilpeläinen, T., 1998: Evolution and 3D modelling of the structural and metamorphic patterns of the Palaeoproterozoic crust in the Tampere-Vammala area, southern Finland. *Geological Survey of Finland, Bulletin 397*, 124 pp.

Korja, A. & Heikkinen, P., 2005: The accretionary Svecofennian orogen-insight from the BABEL profiles. *Precambrian Research 136*, 241–268.

Korja, A., Kosunen, P. & Heikkinen, P., 2009: A case study of lateral spreading: The Precambrian Svecofennian orogen. *Geological Society, London, Special Publications 321*, 225–251.

Korsman, K., 1977: Progressive metamorphism of the metapelites in the Rantasalmi-Sulkava area, southeastern Finland. *Geological Survey of Finland. Bulletin 290*, 82 pp.

Korsman, K., Koistinen, T., Kohonen, J., Wennerström, M., Ekdahl, E., Honkamo, M., Edman, H. & Pekkala, Y., 1997: Bedrock map of Finland 1:1 000 000; Geological Survey of Finland.

Korsman, K., Korja, T., Pajunen, M., Virransalo, P. & GGT/SVEKA Working Group, 1999: The GGT/SVEKA transect: Structure and evolution of the continental crust in the Paleoproterozoic Svecofennian orogen in Finland. *International Geology Review 41*, 287–333.

Kukkonen, I. & Lauri, L., 2009: Modelling the thermal evolution of a collisional Precambrian orogen: High heat production migmatitic granites of southern Finland. *Precambrian Research 168*, 233–246.

Kurhila, M., Andersen, T. & Rämö, O.T., 2010: Diverse sources of crustal granitic magma: Lu–Hf isotope data on zircon in three Paleoproterozoic leucogranites of southern Finland. *Lithos 115*, 263–271.

Kurhila, M., Mänttäri, I., Vaasjoki, M., Rämö, O.T. & Nironen, M., 2011: U–Pb geochronological constraints of the late Svecofennian leucogranites of southern Finland. *Precambrian Research 190*, 1–24.

Kurhila, M., Vaasjoki, M., Mänttäri, I., Rämö, T. & Nironen, M., 2005: U–Pb ages and Nd isotope characteristics of the lateorogenic, migmatizing microcline granites in southwestern Finland. *Bulletin of the Geological Society of Finland 77*, 105–128.

Lahtinen, R., 1996: Geochemistry of Palaeoproterozoic supracrustal and plutonic rocks in the Tampere-Hämeenlinna area, southern Finland. *Geological Survey of Finland, Bulletin 389*, 113 pp.

Lahtinen, R., Huhma, H., Kähkönen, Y. & Mänttäri, I., 2009: Paleoproterozoic sediment recycling during multiphase orogenic evolution in Fennoscandia, the Tampere and Pirkanmaa belts, Finland. *Precambrian Research 174*, 310–336.

Lahtinen, R., Huhma, H. & Kousa, J., 2002: Contrasting source components of the Paleoproterozoic Svecofennian metasediments: Detrital zircon U–Pb, Sm–Nd and geochemical data. *Precambrian Research 116*, 81–109.

Lahtinen, R., Korja, A. & Nironen, M., 2005: Paleoproterozoic tectonic evolution. *In* M. Lehtinen, P. Nurmi & O.T. Rämö (eds.): *Precambrian geology of Finland: Key to the evolution of the fennoscandian shield*, 481–532. Elsevier B.V., Amsterdam, Netherlands.

Lahtinen, R. & Nironen, M., 2010: Paleoproterozoic lateritic paleosol–ultra-mature/mature quartzite–meta-arkose successions in southern Fennoscandia – intra-orogenic stage during the Svecofennian orogeny. *Precambrian Research 183*, 770–790.

Levin, T., Engström, J., Lindroos, A., Baltybaev, S. & Levchenkov, O., 2005: Late-Svecofennian transpressive deformation in SW Finland: Evidence from late-stage D3 structures. *GFF 127*, 129–137.

Ludwig, K.R., 2003: User's Manual for Isoplot 3.00. A Geochronological Toolkit for Microsoft Excel. *Berkeley Geochronology Center, Special Publication 4*, 70 pp.

Mänttäri, I., Aaltonen, I. & Lindberg, A., 2007: U–Pb ages for two tonalitic gneisses, pegmatitic granites, and K-feldspar porphyries, Olkiluoto study site, Eurajoki, SW Finland. *Posiva Working Report 2007–70*, 44 pp.

Mänttäri, I., Talikka, M., Paulamäki, S. & Mattila, J., 2006: U–Pb ages for tonalitic gneiss, pegmatitic granite, and diabase dyke, Olkiluoto study site, Eurajoki, SW Finland. *Posiva Working Report 2006–12*, 18 pp.

Mänttäri, I., Pere, T., Engström, J. & Lahaye, Y., 2010: U–Pb Ages for PGR dykes, KFP, and adjacent older leucosomic PGRs from ONKALO underground research facility, Olkiluoto, Eurajoki, SW Finland. *Posiva Working Report 2010–31*, 52 pp.

Mattila, J., Aaltonen, I., Kemppainen, K., Wikström, L., Paananen, M., Paulamäki, S., Front, K., Gehör, S., Kärki, A. & Ahokas, T., 2008: Geological Model of the Olkiluoto Site, Version 1.0. *Posiva Working Report 2007–92*, 510 pp.
Middlemost, E.A.K., 1994: Naming materials in the magma/igneous rock system. *Earth-Science Reviews 37*, 215–224.
Mouri, H., Korsman, K. & Huhma, H., 1999: Tectono-metamorphic evolution and timing of the melting processes in the Svecofennian Tonalite-Trondhjemite Migmatite Belt: An example from Luopioinen, Tampere area, southern Finland. *Bulletin of the Geological Society of Finland 71*, 31–56.
Mouri, H., Väisänen, M., Huhma, H. & Korsman, K., 2005: Sm–Nd garnet and U–Pb monazite dating of high-grade metamorphism and crustal melting in the West Uusimaa area, southern Finland. *GFF 127*, 123–128.
Nevalainen, J., Väisänen, M., Lahaye, Y. & Fröjdö, S., 2011: LA-MC-ICPMS zircon dating and geochemistry of the intra-orogenic Moisio monzogabbro, Turku, SW Finland. 8th National Geological Colloquium, Helsinki 24–26.10.2011, Helsinki: Abstract Volume. Publications of the Department of Geosciences and Geology, University of Helsinki, C5, 26.
Nironen, M., 1989: Emplacement and structural setting of granitoids in the early Proterozoic Tampere and Savo Schist Belts, Finland: Implications for contrasting crustal evolution. *Geological Survey of Finland, Bulletin 346*, 83 pp.
Nironen, M., 2005: Proterozoic orogenic granitoid rocks. *In* M. Lehtinen, P. Nurmi & O.T. Rämö (eds.): *Precambrian geology of Finland: Key to the evolution of the fennoscandian shield*, 443–479. Elsevier B.V., Amsterdam, Netherlands.
Nironen, M., 2011: The Pyhäntaka formation, southern Finland: A sequence of metasandstones and metavolcanic rocks upon an intra-orogenic unconformity. *Bulletin of the Geological Society of Finland 83*, 5–23.
Nironen, M., Elliott, B.A. & Rämö, O.T., 2000: 1.88–1.87 Ga post-kinematic intrusions of the Central Finland Granitoid Complex: A shift from C-type to A-type magmatism during lithospheric convergence. *Lithos 53*, 37–58.
Nironen, M., Korja, A. & Heikkinen, P., 2006: A geological interpretation of the upper crust along FIRE 2 and FIRE 2A. *Geological Survey of Finland, Special Paper 43*, 77–103.
Nironen, M. & Kurhila, M., 2008: The Veikkola granite area in southern Finland: Emplacement of a 1.83–1.82 Ga plutonic sequence in an extensional regime. *Bulletin of the Geological Society of Finland 80*, 39–68.
Nironen, M. & Mänttäri, I., 2012: Timing of accretion, intra-orogenic sedimentation and basin inversion in the Paleoproterozoic Svecofennian orogen: The Pyhäntaka area, southern Finland. *Precambrian Research 192–95*, 34–51.
Ogenhall, E., 2010: *Geological Evolution of the Supracrustal Palaeoproterozoic Hamrånge Group: A Svecofennian Case Study*, Ph.D. thesis. Acta Universitatis Upsaliensis 738, 53 pp.
Pajunen, M., Airo, M-L., Elminen, T., Mänttäri, I., Niemelä, R., Vaarma, M., Wasenius, P. & Wennerström, M., 2008: Tectonic evolution of the Svecofennian crust in southern Finland. *Geological Survey of Finland, Special Paper 47*, 15–160.
Patchett, J. & Kouvo, O., 1986: Origin of continental crust of 1.9–1.7 Ga age: Nd isotopes and U–Pb zircon ages in the Svecokarelian terrain of South Finland. *Contributions to Mineralogy and Petrology 92*, 1–12.
Peccerillo, R. & Taylor, S.R., 1976: Geochemistry of Eocene calc-alkaline volcanic rocks from the Kastamonu area, northern Turkey. *Contributions to Mineralogy and Petrology 58*, 63–81.
Rosa, D.R.N., Finch, A.A., Andersen, T. & Inverno, C.M.C., 2009: U–Pb geochronology and Hf isotope ratios of magmatic zircons from the Iberian pyrite belt. *Mineralogy and Petrology 95*, 47–69.
Rutanen, H., Andersson, U.B., Väisänen, M., Johansson, Å., Fröjdö, S., Lahaye, Y. & Eklund, O., 2011: 1.8 Ga magmatism in southern Finland: Strongly enriched mantle and juvenile crustal sources in a post-collisional setting. *International Geology Review 53*, 1622–1683.
Rutland, R.W.R., Williams, I.S. & Korsman, K., 2004: Pre-1. 91 Ga deformation and metamorphism in the Palaeoproterozoic Vammala Migmatite Belt, southern Finland, and implications for Svecofennian tectonics. *Bulletin of the Geological Society of Finland 76*, 93–140.
Saalmann, K., Mänttäri, I., Ruffet, G. & Whitehouse, M.J., 2009: Age and tectonic framework of structurally controlled Palaeoproterozoic gold mineralization in the Häme belt of southern Finland. *Precambrian Research 174*, 53–77.
Schreurs, J. & Westra, L., 1986: The thermotectonic evolution of a Proterozoic, low pressure, granulite dome, West Uusimaa, SW Finland. *Contributions to Mineralogy and Petrology 93*, 236–250.
Selonen, O. & Ehlers, C., 1998: Structural observations on the Uusikaupunki trondhjemite sheet, SW Finland. *GFF 120*, 379–382.
Selonen, O., Ehlers, C. & Lindroos, A., 1996: Structural features and emplacement of the late Svecofennian Perniö granite sheet in southern Finland. *Bulletin of the Geological Society of Finland 68*, 5–17.
Skyttä, P. & Mänttäri, I., 2008: Structural setting of late Svecofennian granites and pegmatites in Uusimaa Belt, SW Finland: Age constraints and implications for crustal evolution. *Precambrian Research 164*, 86–109.
Skyttä, P., Väisänen, M. & Mänttäri, I., 2006: Preservation of Palaeoproterozoic early Svecofennian structures in the Orijärvi area, SW Finland: Evidence for polyphase strain partitioning. *Precambrian Research 150*, 153–172.
Stacey, J.S. & Kramers, J.D., 1975: Approximation of terrestial lead isotope evolution by a two-stage model. *Earth and Planetary Science Letters 26*, 207–221.
Stålfors, T. & Ehlers, C., 2006: Emplacement mechanisms of Late-orogenic granites - Structural and geochemical evidence from southern Finland. *International Journal of Earth Sciences 95*, 557–568.
Sun, S.-S. & McDonough, W.F., 1989: Chemical and isotopic systematics of oceanic basalts: Implications for mantle composition and processes. *Geological Society, London, Special Publications 42*, 313–345.
Suominen, V., 1987: Korppoo. Geological map of Finland 1:100 000: Pre-Quaternary rocks, sheet 1032. Survey of Finland, Espoo.
Suominen, V., 1991: The chronostratigraphy of southwestern Finland with special reference to Postjotnian and Subjotnian diabases. *Geological Survey of Finland, Bulletin 356*, 100 pp.
Suominen, V. & Torssonen, M., 1993: Rauma. Geological map of Finland 1:100 000: Pre-Quaternary rocks, sheet 1132, Espoo, Geologian tutkimuskeskus.
Torvela, T. & Ehlers, C., 2010: From ductile to brittle deformation: Structural development and strain distribution along a crustal-scale shear zone in SW Finland. *International Journal of Earth Sciences 99*, 1133–1152.
Torvela, T., Mänttäri, I. & Hermansson, T., 2008: Timing of deformation phases within the South Finland shear zone, SW Finland. *Precambrian Research 160*, 277–298.
Turner, S., Arnaud, N., Liu, J., Rogers, N., Hawkesworth, C., Harris, N., Kelley, S., van Calsteren, P. & Deng, Q., 1996: Post-collision, shoshonitic volcanism on the Tibetan plateau: Implication for convective thinning of the lithosphere and source of ocean island basalts. *Journal of Petrology 37*, 45–71.
Vaasjoki, M. & Sakko, M., 1988: The evolution of the Raahe-Ladoga zone in Finland: Isotopic constraints. *Geological Survey of Finland, Bulletin 343*, 7–32.
Väisänen, M. & Hölttä, P., 1999: Structural and metamorphic evolution of the Turku migmatite complex, southwestern Finland. *Bulletin of the Geological Society of Finland 71*, 177–218.
Väisänen, M., Johansson, Å., Andersson, U.B., Eklund, O. & Hölttä, P., 2012: Palaeoproterozoic adakite- and TTG-like magmatism in the Svecofennian orogen, SW Finland. *Geologica Acta 10*, in press. DOI:10.1344/105.000001761.
Väisänen, M. & Kirkland, C.L., 2008: U–Th–Pb geochronology of igneous rocks in the Toija and Salittu Formations, Orijärvi area, southwestern Finland: Constraints on the age of volcanism and metamorphism. *Bulletin of the Geological Society of Finland 80*, 73–87.
Väisänen, M., Mänttäri, I. & Hölttä, P., 2002: Svecofennian magmatic and metamorphic evolution in southwestern Finland as revealed by U–Pb zircon SIMS geochronology. *Precambrian Research 116*, 111–127.
Väisänen, M., Mänttäri, I., Kriegsman, L.M. & Hölttä, P., 2000: Tectonic setting of post-collisional magmatism in the Palaeoproterozoic Svecofennian Orogen, SW Finland. *Lithos 54*, 63–81.
Väisänen, M. & Skyttä, P., 2007: Late Svecofennian shear zones in southwestern Finland. *GFF 129*, 55–64.
Van Duin, J.A., 1992: *The Turku Granulite Area, SW Finland: A Fluid-Absent Svecofennian Granulite Occurrence*. Ph.D. thesis. Vrije Universiteit, Amsterdam, Holland, 234 pp.
Verma, S.P., Torres-Alvarado, I.S. & Sotelo-Rodríguez, Z.T., 2002: SINCLAS: Standard igneous norm and volcanic rock classification system. *Computers & Geosciences 28*, 711–715. http://www.sciencedirect.com/science/article/pii/S0098300401000875-CORR1.
Woodard, J., 2010: *Genesis and Emplacement of Carbonatites and Lamprophyres in the Svecofennian Domain*. Ph.D. thesis. Annales Universitas Turkuensis, Ser. A II. Tom. 252. University of Turku, 50 pp.